

AD-756 706

DRIVING-POINT-IMPEDANCE MEASUREMENT AND
BALUN DESIGN FOR SPIRAL ANTENNAS

William B. Weir, et al

Stanford Research Institute

Prepared for:

Department of State

March 1972

DISTRIBUTED BY:

NTIS

National Technical Information Service
U. S. DEPARTMENT OF COMMERCE
5285 Port Royal Road, Springfield Va. 22151

AD 756706

Final Report — Task A

**DRIVING-POINT-IMPEDANCE MEASUREMENT
AND BALUN DESIGN FOR SPIRAL ANTENNAS**

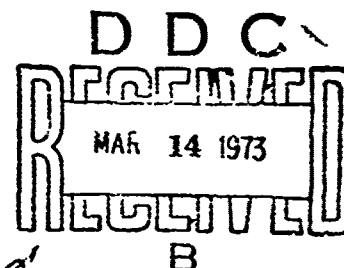
By: WILLIAM B WEIR LLOYD A. ROBINSON

Prepared for:

DEPARTMENT OF STATE
OFFICE OF SECURITY, ROOM 3810A
21st AND VIRGINIA AVENUE
WASHINGTON, D.C. 20520

CONTRACT 1038-101649-SCC-10507

Reproduced by
NATIONAL TECHNICAL
INFORMATION SERVICE
U.S. Department of Commerce
Springfield, VA 22151



STANFORD RESEARCH INSTITUTE
Menlo Park, California 94025 • U.S.A.

DISTRIBUTION STATEMENT A

Approved for public release;
Distribution Unlimited



STANFORD RESEARCH INSTITUTE
Menlo Park, California 94025 · U.S.A

Final Report — Task A

March 1972

DRIVING-POINT-IMPEDANCE MEASUREMENT AND BALUN DESIGN FOR SPIRAL ANTENNAS

By: WILLIAM B WEIR LLOYD A. ROBINSON

Prepared for:

DEPARTMENT OF STATE
OFFICE OF SECURITY, ROOM 3810A
21st AND VIRGINIA AVENUE
WASHINGTON, D.C. 20520

CONTRACT 1038-101649-SCC-10507

SRI Project 1370

Approved by:

CHARLES J. SHOENS, *Director*
Electromagnetic Techniques Laboratory

RAY L. LEADABRAND, *Executive Director*
Electronics and Radio Sciences Division

Copy No. 25

ABSTRACT

Measured impedance data are presented for two planar, equiangular, printed-circuit, two-arm, spiral antennas not mounted over cavities. The impedance was measured at the center terminals of the antennas when the antennas were placed against various types of building materials and when situated in free space. Measurements were made at frequencies both within and below the radiating frequency band of each antenna. Compact baluns with flat form factors were designed to match the average antenna impedance over the radiating frequency band found from these measurements, to an unbalanced 50-ohm impedance. The measured impedance and loss characteristics of the compact baluns, data showing the effect on antenna impedance of running a twin-lead transmission line close to the antenna, and impedance data for two complete balun/antenna configurations in free space are also presented.

It is shown that the center-driven impedance is significantly lower than the theoretical impedance of 188.5 ohms due to the presence of the dielectric that supports the spirals and due to the fact that the ideal spiral geometry close to the center feed terminals was not realized. It is also shown, however, that the presence of various types of building materials does not affect this impedance significantly over the radiating frequency bands of the antennas.

Two compact baluns were designed that matched the antennas to an unbalanced 50-ohm-system impedance with VSWR's less than 1.5 over most of the radiating frequency band of each antenna. This match was extended to frequencies below the radiating frequency band by terminating the outer end of the antennas with combination lumped and distributed loads.

To achieve a practical, low-profile configuration that included both antenna and balun, it was necessary to position the balun in the plane of the antenna. Impedance measurements of such a configuration revealed some degradation in the match between the antenna and 50 ohms.

CONTENTS

ABSTRACT	iii
LIST OF ILLUSTRATIONS.	vii
LIST OF TABLES	xi
ACKNOWLEDGMENTS.	xiii
 I INTRODUCTION.	 1
A. Background	1
B. Objectives	2
C. Method of Approach	2
 II MEASUREMENT TECHNIQUE	 5
A. Equipment Configuration for Measurement Setup.	5
B. Design of Balanced Calibration Standards and Terminations	7
 III DRIVING-POINT-IMPEDANCE DATA FOR ANTENNAS IN THE PRESENCE OF VARIOUS BUILDING MATERIALS.	 15
A. General.	15
B. Discussion of Self-Complementary Spiral-Antenna Characteristics.	17
1. Electrical Properties	17
2. Transmission-Line Analogy	18
C. Description of Building Materials and Antenna Orientations	19
D. Driving-Point-Impedance Characteristics of Antennas	20
1. Data for the 24-Inch Antenna.	20
2. Discussion of Characteristics	32
a. Impedance.	32
b. Cutoff Frequencies	37
3. Data for the 12-Inch Antenna.	41

IV	DRIVING-POINT IMPEDANCE OF A SPIRAL ANTENNA FED BY A TWO-WIRE TRANSMISSION LINE.	49
V	DESIGN OF THE COMPACT BALUN	59
	A. Theory	59
	B. Choice of Parameters	65
	C. Measured Characteristics	67
VI	INPUT-IMPEDANCE AND REFLECTION DATA FOR COMPACT BALUN/ANTENNA CONFIGURATIONS IN FREE SPACE.	71
	A. General.	71
	B. Balun/Antenna Configuration.	72
	C. Termination for the Antenna Outer Ends	75
	D. Measured Data for the Balun/Antenna Configurations	82
VII	SUMMARY AND CONCLUSIONS	99
	REFERENCES	103

ILLUSTRATIONS

Figure II-1	Balun Terminations Used to Obtain System Calibration Data	9
Figure II-2	132-ohm-Load Termination	12
Figure III-1	Driving-Point Impedance and Reflection Data at the Center of the 24-Inch Spiral Antenna in Free Space	21
Figure III-2	Smith-Chart Plot for 24-Inch Spiral Antenna Fed at the Center with a 200-ohm-Impedance Generator.	22
Figure III-3	Driving-Point Impedance of the 24-Inch Spiral Antenna Placed in Juxtaposition with Several Types of Dielectric Building Materials	26
Figure III-4	Driving-Point Impedance of the 24-Inch Spiral Antenna Placed Against Glass and Canvas.	30
Figure III-5	Cross-Section View of Spiral Antenna Depicting Interaction of Non-Radiating Fields with Dielectric Building Material Brought in Close Contact with Antenna	34
Figure III-6	Current Relationships on a Spiral Antenna.	38
Figure III-7	Driving-Point Impedance and Reflection Data at the Center of the 12-Inch Spiral Antenna in Free Space.	42
Figure III-8	Smith-Chart Plot for 12-Inch Spiral Antenna Fed at the Center with a 200-ohm Impedance Generator.	43
Figure III-9	Driving-Point Impedance of the 12-Inch Spiral Antenna Placed in Juxtaposition with Several Types of Dielectric Building Materials	44

Figure IV-1	Cross-Section View of Antenna/Transmission-Line-Fed Configuration.	50
Figure IV-2	Driving-Point Impedance of the 12-Inch Spiral Antenna in Free Space Fed by Means of a Balanced Two-Wire Transmission Line	52
Figure V-1	Equivalent Circuit for the Compact Balun	59
Figure V-2	Compact Balun.	63
Figure V-3	Smith-Chart Impedance Plot for Compact Baluns Terminated in a Matched 132-ohm Load	65
Figure V-4	Real and Imaginary Parts of Input Impedance of the Compact Baluns Terminated in a Matched 132-ohm Load	69
Figure V-5	Reflection Data and Transmission Loss for the Compact Baluns Terminated in a Matched 132-ohm Load	70
Figure VI-1	Compact Balun Attached to Outer Metal Ring of 12-Inch Antenna.	75
Figure VI-2	Calculated Performance of Matching Networks for 12-Inch-Antenna Outer Ends	78
Figure VI-3	Driving-Point Impedance of the Center of the 12-Inch Spiral Antenna When the Outer Ends Are Terminated with $n = 4$ Networks	80
Figure VI-4	Impedance and Reflection Data at the Unbalanced Terminal of the Compact Balun Connected to the 24-Inch Spiral Antenna by Means of a Transmission Line Perpendicular to the Antenna.	84
Figure VI-5	Smith-Chart Plot of the Impedance Data of Figure VI-4.	85
Figure VI-6	Impedance and Reflection Data at the Unbalanced Terminal of the Compact Balun Connected to the 24-Inch Spiral Antenna by Means of a Transmission Line Parallel to and Touching the Antenna.	86

Figure VI-7	Smith-Chart Plot of the Impedance Data of Figure VI-6.	87
Figure VI-8	Impedance and Reflection Data at the Unbal- anced Terminal of the Compact Balun Connected to the 12-Inch Spiral Antenna by Means of a Transmission Line Perpendicular to the Antenna.	88
Figure VI-9	Smith-Chart Plot of the Impedance Data of Figure VI-8.	89
Figure VI-10	Impedance and Reflection Data at the Unbal- anced Terminal of the Compact Balun Connected to the 12-Inch Spiral Antenna by Means of a Transmission Line Parallel to and Touching the Antenna.	90
Figure VI-11	Smith-Chart Plot of Impedance Data of Figure VI-10	91

TABLES

Table IV-1	Maximum Values of VSWR Occurring in the Radiating Frequency Band of the 12-Inch Antenna for Several Antenna/Transmission-Line Configurations	56
Table V-1	Comparison of Turns Ratios.	66
Table VI-1	Peak VSWR and System Sensitivity Loss for Several 24-Inch Antenna Configurations.	94
Table VI-2	Peak VSWR and System Sensitivity Loss for Several 12-Inch Antenna Configurations.	95

Preceding page blank

ACKNOWLEDGMENTS

The authors wish to acknowledge the engineering assistance of Mr. Allen Podell who designed the low-profile, compact coils and the experimental support provided by Mr. York Sato who obtained the many impedance measurements required for this report.

The technical contract monitors for this contract were Mr. Theodore H. Tea and Mr. Evelyn Kusser, Research and Development Branch, Division of Technical Services, Office of Security, Department of State.

Preceding page blank

I INTRODUCTION

A. Background

The study reported herein is a follow-on to Contract 1083-100623-SCC-09824 (SRI Project 1081).^{1*} The objective of that contract was to measure the impedance at the outside ends of two spiral antennas and to design matching networks that could be connected between the spiral outer ends and the surrounding metal ring of the antennas to reduce the low-frequency VSWR at the spiral centers. The results obtained from that contract were used in the current study, which is reported herein.

The current study is divided into two tasks. Task A, the subject of this report, is involved with the driving-point impedance[†] measurements of the two spiral antennas used in the former study, and the subsequent design of two compact baluns with flat form factors used to match the antennas to a receiver system with a 50-ohm unbalanced input impedance. Task B, which will be the subject of a separate report, is involved in the design and construction of two loop antennas that will operate in the frequency range from 10 MHz up to the low-frequency radiation cutoff of their respective spiral antennas. Each of these loop antennas will be mounted concentrically with one of the spiral antennas.

* References are listed at the end of the report.

[†] The impedance at the terminals at the center of the antennas, where this type of antenna is normally driven.

The antennas used in Task A were supplied by the Department of State and are planar, equiangular, printed-circuit, two-arm, spiral antennas not mounted over cavities. These antennas are the Electro/Data Models AN15-12 and AN15-24, each Serial Number 1. One antenna is 12 inches in diameter across the spiral ends and the other is 24 inches in diameter. Other details are described in the previous report under Contract 1083-100623-SCC-09824.¹

B. Objectives

An objective of Task A was to determine the driving-point impedance within the radiating frequency range of each spiral antenna when situated in free space and when backed by various typical dielectric building materials. An average was taken of the impedances measured for each combination of antenna and building material, and in free space. A second objective was to design two flat-form-factor, compact baluns to match this average driving-point impedance to a system with an unbalanced, 50-ohm impedance.

The final objective was to investigate several balun/antenna configurations to determine which configuration minimized the VSWR and at the same time maintained a low-profile balun/antenna configuration. As part of the final objective, the use of matching networks to terminate the outer ends of the spirals was investigated to extend the low VSWR to frequencies below the radiating band. The matching networks accomplish this by absorbing the currents reaching the outer ends of the antennas.

C. Method of Approach

Impedance measurements were made using the computer-controlled Hewlett-Packard automatic network analyzer owned by the Institute. The network analyzer measured the reflection coefficient relative to its

own impedance. From these data, complex impedance and VSWR are determined by the computer associated with the network analyzer and either plotted as a function of frequency on oscilloscopes and a recorder, or listed on a teletype terminal, or both.

In order to measure the impedance at the center terminals of each spiral, a measurement instrument is needed with a balanced port. The unbalanced reflection port of the network analyzer was converted to a balanced port using a balun (BALanced-to-UNbalanced mode transformer). The network analyzer was then calibrated using reflection standards at the balanced port. The result is that the balun characteristics were calibrated out of the measured data, and the output data are the actual driving-point impedances of the antennas.

Using the results of the antenna impedance measurements, the compact baluns were designed. The characteristics of each balun when terminated in a balanced resistive load were measured using the conventional unbalanced port of the network-analyzer balun. As one step in deciding how to mount the baluns on the antennas, a study was made on the effects, on driving-point impedance, of running a twin-lead transmission line close to the antenna surface. The final measurements obtained for this report were made on two complete compact balun/antenna configurations. Impedance was measured at the unbalanced port of the balun when it was connected to its respective antenna situated in free space. During these measurements the outer ends of the antenna spiral conductors were terminated with networks designed to improve the antenna input match at frequencies below the radiating band of each antenna. The results from Contract 1083-100623-SCC-09824 were used as an aid in designing these outer terminations.

II MEASUREMENT TECHNIQUE

A. Equipment Configuration for Measurement Setup

The measurements described in this report were made using the Hewlett-Packard 8541A automatic network analyzer. This instrument specifically measured the scattering parameters^{*} of microwave networks. From these parameters, various electrical properties of the microwave networks can be derived. For example, VSWR and Smith-chart plots may be found from scattering-parameter data, and if the system impedance (source impedance) under which the measurements were obtained is known, the real and imaginary components of the network input impedance may be derived. Processing of measured data is done by the network-analyzer computer, which also provides automatic system-control functions. A significant feature of the automatic network analyzer is that system errors may be determined by measuring standard components with known electrical properties.² By use of the computer these errors are subsequently calibrated out of the measured scattering parameters of the microwave network, the electrical properties of which are unknown.³

Using the automatic network analyzer, the driving-point impedance as seen at the center feed terminals of the 12-inch and 24-inch spiral antenna were measured over a range of frequencies. To obtain impedance measurements the reflection-measurement port of the network analyzer was connected to a 4:1 impedance balun transformer which in turn was connected either directly to the antenna or to the antenna through a

* Complex reflection and transmission coefficients.

balanced 150-ohm transmission line. The balun^{*} was required to convert the two unbalanced output currents from the network-analyzer coaxial reflection port to the two balanced currents (equal amplitude but opposite in phase) required to excite the antenna. The balun impedance-transformation ratio need not have been 4:1, however; any other practically achievable ratio could have been used as long as its value was known. The impedance-transformation ratio determines the system (or source) impedance under which the measurements were obtained. Knowledge of system impedance is necessary in order to correctly interpret the measurement data or, specifically, to compute the correct driving-point impedance from reflection-coefficient data.³ (The 4:1 Anzac balun impedance transformer transformed the network-analyzer-system impedance of 50 ohms to 200 ohms.)

The balanced output port of the balun was modified in order that it could be directly connected to the 24-inch antenna. This modification consisted of extending the balanced output port using a rigid-wire, 200-ohm transmission line with wire spacing equal to the 24-inch-antenna feed-point spacing of 300 mils.[†] An additional tapered 200-ohm transmission line was built. In order that the same balun could be used for the 12-inch-antenna impedance measurements, the spacing between the two wires of this line was tapered from 300 to 150 mils. The characteristic impedance of 200 ohms was maintained over the length of the transmission line by tapering the wire diameter appropriately.

A compact balun with a flat form factor was built for each spiral antenna. As will be explained in Section V, the baluns were designed

* Anzac TKN-6360-N, Serial No. 485, furnished by the sponsor.

† The wire diameter was 113 mils to give a characteristic impedance of 200 ohms for the transmission line.

to transform an unbalanced source impedance of 50 ohms to a balanced real impedance equal to the average driving-point impedance within the radiation band of the 12-inch and 24-inch antennas (see Section III). The electrical properties of each compact balun, presented in Section V, were measured using the network analyzer. Reflection-coefficient measurements (from which VSWR is determined) were obtained when the balanced output port of the baluns were terminated with a load equal to the average driving-point impedance of the antennas. In addition, the balun loss was measured. This measurement required two additional balun terminations--a short and an open.⁴ A description and construction details of these balanced terminations as well as the balanced load appear in the following subsection.

Once the final design and construction of the compact baluns were completed, they were connected to their respective antennas by means of a 132-ohm transmission line. The final measurements reported herein were made on the compact balun/antenna configuration. Impedance measurements were made looking into the unbalanced input port of the balun. No special calibration considerations were necessary for these last measurements. The reflection port of the network analyzer to which the balun was connected during measurement is an unbalanced 50-ohm-impedance port. System calibration was accomplished using the Hewlett-Packard standard terminations supplied with the network analyzer.

B. Design of Balanced Calibration Standards and Terminations

As explained above, a balun was added to the network-analyzer reflection-measurement port to convert it to a balanced port. To obtain an accurate measurement of the unknown driving-point impedance of the antenna, the balun characteristics as well as the network-analyzer-system errors must be measured in order that these quantities can be

subtracted out of the antenna data. This required that system calibration be accomplished by measuring known standards connected to the balanced (output) port of the balun. None of the standards supplied with the network analyzer by Hewlett-Packard could be used, since they fit only coaxial connectors.* Hence, three balanced standards used for system calibration were built at SRI and are described as follows.

The three standard terminations together with the Anzac balun used on the network analyzer are shown in Figure II-1. Each termination is connected directly to the 200-ohm rigid-wire transmission line that extends the balanced output port of the balun. The 200-ohm-load termination consists of two 100-ohm carbon resistors connected in series. Each resistor was selected so that when connected in series they would match the characteristic impedance of the transmission line as closely as possible.[†] One end of each resistor is soldered to a female pin that plugs onto the end of the balun transmission line. The female pins were taken from type BNC connectors. The other end of each resistor was embedded within a metal block, as shown in Figure II-1. The physical configuration of the load--specifically, the angle between the two resistors, and the depth at which each resistor is inserted into the block--was adjusted empirically to minimize load reactance. Adjustments were made after the impedance of each 100-ohm resistor was measured

* S- and X-band waveguide standards, as well as standards that fit a special Hewlett-Packard jig used for transistor measurements, are also available. These also are of no use in the application being discussed.

[†] This termination should be a very-low-reflection load; for a discussion of the three types of standard terminations required for system calibration and the mathematical procedures in determining system errors, see Ref. 2.

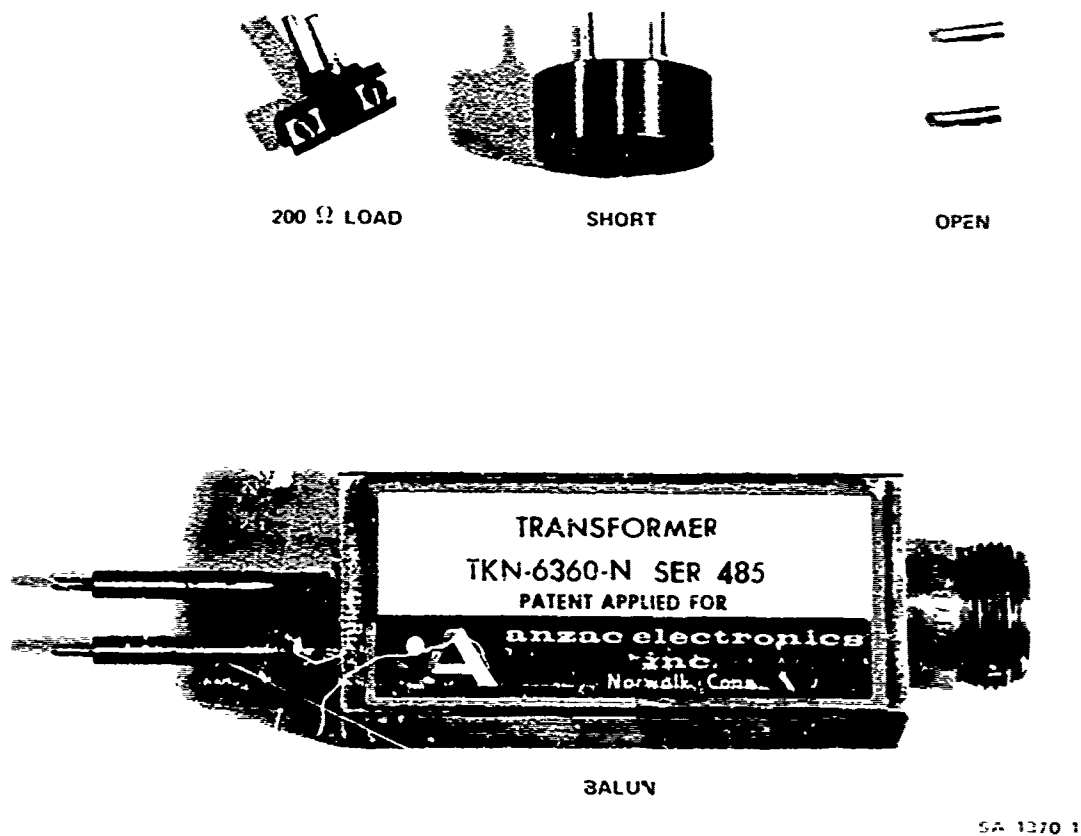


FIGURE II-1 BALUN TERMINATIONS USED TO OBTAIN SYSTEM CALIBRATION DATA. From upper left to upper right are shown the 200-ohm load, and the short and the open terminations, the Anzac balun is shown below the terminations.

separately over a ground plane. Measuring each resistor individually allowed use of the network analyzer in obtaining the load impedance. Since the termination is a balanced load, a virtual ground exists at the plane of symmetry (provided that the resistors are essentially equal). Thus, for measurement purposes each resistor can be mounted over a ground plane, and then connected directly to the coaxial reflection measurement port of the network analyzer.* The total load impedance was found by adding the impedances of the two 100-ohm resistors. The final load configuration was found to have a VSWR of less than 1.03, with respect to a 200-ohm system, over the frequency range from 100 to 2000 MHz.

The two additional standards shown in Figure II-1 are the short-circuit and open-circuit terminations. The short circuit consists of two BNC pins attached perpendicular to a metal block. The pins are identical in length, diameter, and spacing to those used for the 200-ohm-load termination. The reference plane[†] to which the driving-point impedance data presented in the next section refer, is defined by the plane metal surface connected to the pins. The plane surface of the metal block was made large enough that essentially all of the fields about the transmission line terminate on it.

The open circuit simply consists of two BNC pins attached to the Anzac balun. These pins are again identical to those used for the other two standard terminations, so that the open circuit occurs at the reference plane defined by the short-circuit termination. Because of

* Calibration for these measurements was completed using Hewlett-Packard coaxial standards connected to the network analyzer reflection port.

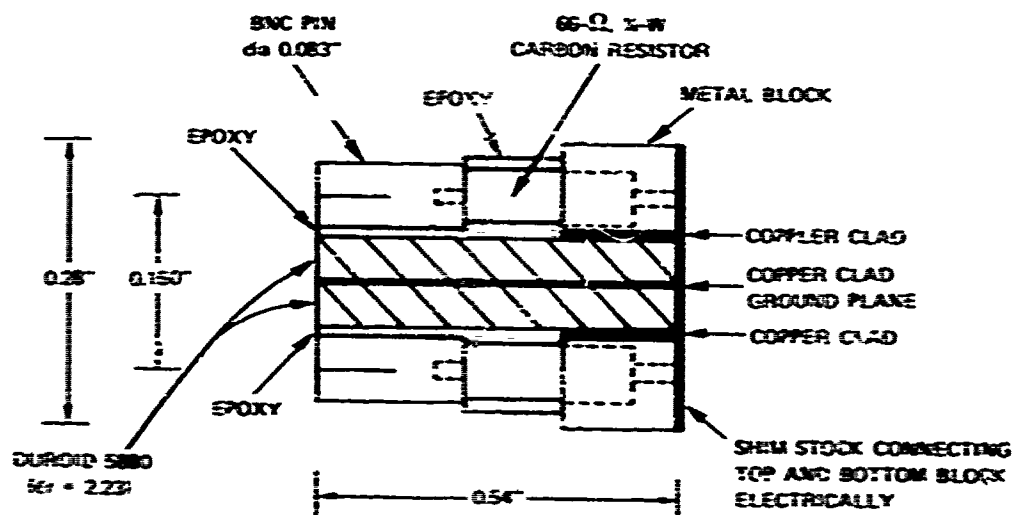
† Specifically, the plane at which phase comparisons of the incident and reflected waves are made.

fringing capacitance at the open end of the pins, the open-circuit termination does not appear as a perfect open circuit. However, the fringing capacitance at the open end of the pins⁵ was computed, and the calibration data were corrected accordingly.*

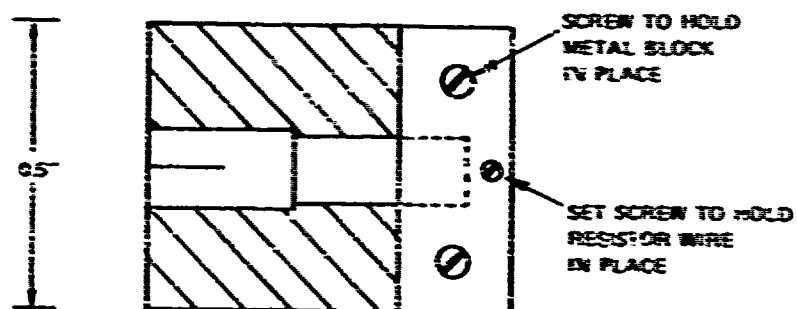
In addition to the calibration standards just described, three terminations of known characteristics were needed to measure the electrical properties of the compact baluns designed at SRI. Like the calibration standards, these terminations were a very-low-reflection resistive load, a short circuit, and an open circuit.⁴ A sketch of the resistive load is shown in Figure II-2. The load is similar to the calibration-standard load described above, in that it is a balanced load consisting of two carbon resistors connected in series. However, the impedance requirements are different, since the compact baluns required a 132-ohm termination for its very-low-reflection load.⁺ As shown in Figure II-2, two selected 66-ohm resistors are each supported by a metal block and are connected in series by shorting each block together. The other end of each resistor is connected to a separate SMC pin, and these pins are spaced 150 mils apart. The two pins form a transmission line with a characteristic impedance of 144 ohms in free space. Two pieces of dielectric material were inserted between the pins to reduce the characteristic impedance to 132 ohms. Each piece of dielectric was copper clad on one side and put together so that the copper-clad sides pressed against each other, forming a ground plane as shown in

* See Eqs. (8) through (10), Ref. 2. Note that Eq. (8) of Ref. 2 should read $\alpha = 2 \tan^{-1} (0.0003142 \cdot F \cdot C)$.

⁺ The 132-ohm impedance is the real part of the average driving-point impedance of both antennas in their radiating frequency bands as determined by the measurements discussed in Section III.



132-a CROSS-SECTION VIEW



132-b TOP VIEW

SA-1370-2

FIGURE II-2 132-a LOAD TERMINATION

Figure II-2. As was done with the calibration-standard load, each resistor in the compact-balun load was measured separately with the network analyzer by connecting a coaxial-connector center pin to a resistor RVC pin and the outer conductor of the connector to the ground plane. The depth of each resistor in its supporting metal block was adjusted to minimize reactance. When the measurements for each resistor were combined, the total VSWR of the final load configuration, referenced to 132 ohms, was less than 1.04 over the frequency range from 100 to 1500 MHz, and less than 1.08 up to 2000 MHz.

The short-circuit and open-circuit terminations used in measuring the electrical properties of the compact baluns differed physically from the calibration standards described above only in their pin spacing. The pin spacing was 150 mils, and the pins were surrounded by dielectric material to lower their characteristic impedance to 132 ohms.

III DRIVING-POINT-IMPEDANCE DATA FOR ANTENNAS IN THE PRESENCE OF VARIOUS BUILDING MATERIALS

A. General

The data presented in this section show the results of driving-point-impedance measurements in the 100-to-1500-MHz frequency range for the 12-inch and 24-inch spiral antennas obtained when the antennas were in juxtaposition with various types of dielectric building materials. Driving-point impedance is defined here as the input impedance looking into the center-feed terminals where spiral antennas are usually driven. The purpose in making these measurements was to find an average, real driving-point impedance for all the antenna-and-building-material combinations considered in the report. Subsequent to these measurements, a compact balun, described in Section V, was designed for each antenna to match this average driving-point impedance (balanced) to an unbalanced source impedance of 50 ohms.

In this report only the primary current mode generated on the spiral antenna is considered. In general, many current modes can exist, depending on the electrical size of the antenna.⁶ However, within the frequency range over which antenna measurements were made, the primary mode was the dominant mode of radiation. When several modes are excited simultaneously, the angular region of radiation is different for each. When moving from the center of the antenna outward along the spiral conductors, the primary-mode radiation region is reached first, the secondary mode radiation region next, etc. Hence, at frequencies where the primary mode and secondary or higher-order modes exist simultaneously, most of the energy in the primary mode is first radiated, leaving an insignificant amount of energy in the higher-order modes to be

radiated further along the spiral conductors. As frequency is increased, of course, the primary-mode radiation region moves closer to the center of the spiral until the feed terminals are reached. At this point, the primary-mode upper radiating-frequency limit (or higher-frequency cutoff) is reached and the secondary mode becomes the dominant mode of radiation. Thus, in the following discussions, the radiating-frequency range of the spiral antennas is defined and the antenna characteristics are explained in terms of the primary mode of radiation only.

In obtaining the driving-point impedance data for the spiral antennas, no particular attention was given to how the outer ends of the spiral antennas were terminated.* This was because the results from the previous contract, under which various ways of terminating the spiral antennas were investigated, showed that any termination could be used without affecting the driving-point impedance within the radiating-frequency range of the antennas.¹ The upper radiating-frequency limit is primarily determined by the finite antenna-feed-point spacing, whereas the lower limit is determined by the outer radius of the spiral. The average driving-point impedance found for each spiral antenna was determined only from data obtained within these frequency limits. Below the lower radiation-frequency limit, driving-point impedance is extremely erratic unless the antenna outer ends are properly terminated. If they are, the driving-point impedance is also relatively constant down to the lower frequencies, but in any case the frequency limits for good radiation are unaffected.

* The ends of the spirals were left essentially as they were for the former contract (Ref. 1); the ends of the 24-inch spiral were left open and the ends of the 12-inch spiral were shorted to the outer antenna metal support ring.

B. Discussion of Self-Complementary Spiral-Antenna Characteristics

1. Electrical Properties

To interpret the driving-point-impedance data presented in this section as well as the data presented in subsequent sections, knowledge of the general frequency characteristics of self-complementary spiral antennas^{7,8} is necessary. These antenna characteristics are now summarized below.

The frequency band for good radiation is determined by the physical dimensions of the antenna. Radiation occurs in an annular region with average circumference of one wavelength at the frequency of excitation. Since any physically realizable antenna has finite size, its radiating-frequency band will be limited. The upper frequency limit of the radiating band is determined by the finite center-feed-terminal spacing, since at the feed points the spiral elements end abruptly. As the excitation frequency is lowered, the radius of the radiating region increases until it reaches the outer ends of the spiral elements. At this point the lower frequency limit of the radiating band is reached.

Within the radiating frequency band of the antenna the driving-point impedance is constant and has a theoretical value of approximately 188 ohms in free space.* If the frequency is increased through the upper radiating-frequency limit, erratic behavior of driving-point impedance is expected during the transition from the primary to the secondary mode of radiation. If the frequency is decreased below the lower frequency limit, currents are reflected from the outer ends of the spiral.

* This assumes an infinite spiral and that the electric fields extend only into free space (i.e., no field interaction with the dielectric support of the spiral, which would lower the impedance).

This causes high VSWR and erratic behavior with variation in frequency of the driving-point impedance. This erratic behavior at the lower frequencies may be alleviated somewhat by properly terminating the outer ends of the spiral such that the low-frequency currents are absorbed rather than reflected. Extending the frequency range for constant driving-point impedance is important in some applications.

In practice, spiral antennas have dielectric material backing for support (typical are printed-circuit spiral antennas). The presence of the dielectric material will lower the driving-point impedance by an amount that depends on the dielectric constant and on the ratio of dielectric thickness to conductor spacing at the center of the antenna. Generally, the presence of the dielectric material will also lower both frequency limits of the radiating band, but since the ratio of dielectric thickness to conductor spacing is usually small at the outside of the spiral compared to that ratio at the antenna center, the lower frequency limit will remain virtually unchanged. These characteristics will be discussed in more detail later.

2. Transmission-Line Analogy

The spiral antenna, driven at its center, may be thought of as a kind of transmission line, consisting of spiral stripline conductors, terminated in the antenna radiation resistance. This analogy may be explained by the fact that the current distribution along adjacent spiral conductors is approximately 180° out of phase except in the annular region where the antenna is radiating. In this region the currents are approximately in phase. Thus, from the center of the spiral to the radiating region, two adjacent spiral conductors act like a transmission line terminated in the radiating region, which acts as an antenna radiation resistance. The radiation resistance is matched to this equivalent transmission line in the sense that most of the

energy traveling along the line is radiated into free space from the radiating region of the antenna.

To carry this analogy further, it is seen that the length of the equivalent transmission line is variable, depending on frequency. At the lower radiating-frequency limit, the length is maximum and is equal to the path length of the spiral conductors from the center-feed terminals to the outer ends. Below the low-frequency limit the radiation resistance effectively becomes infinite and all the energy traveling down the equivalent transmission line is reflected back to the source (i.e., the center-feed terminals).

With the aid of this analogy it is seen that the spiral antenna excites two types of electric fields within the radiating-frequency range of the antenna. The radiating fields are of one type; energy in these fields is radiated into free space or, analogously, dissipated into the antenna radiation resistance. The other fields are transmission-line-like fields, which extend from one adjacent spiral conductor to the other. These fields, interacting with the dielectric media about the antenna, determine the characteristic impedance of the equivalent transmission line and, furthermore, determine the wavelength of the frequency of excitation. This characteristic impedance is equal to the transmission-line input impedance, or, analogously, to the spiral-antenna driving-point impedance, when the transmission line is terminated in a matched load (the antenna radiation resistance in this analogy). The transmission-line-type fields responsible for the characteristic impedance of the equivalent transmission line are termed the "non-radiating" fields in this report.

C. Description of Building Materials and Antenna Orientations

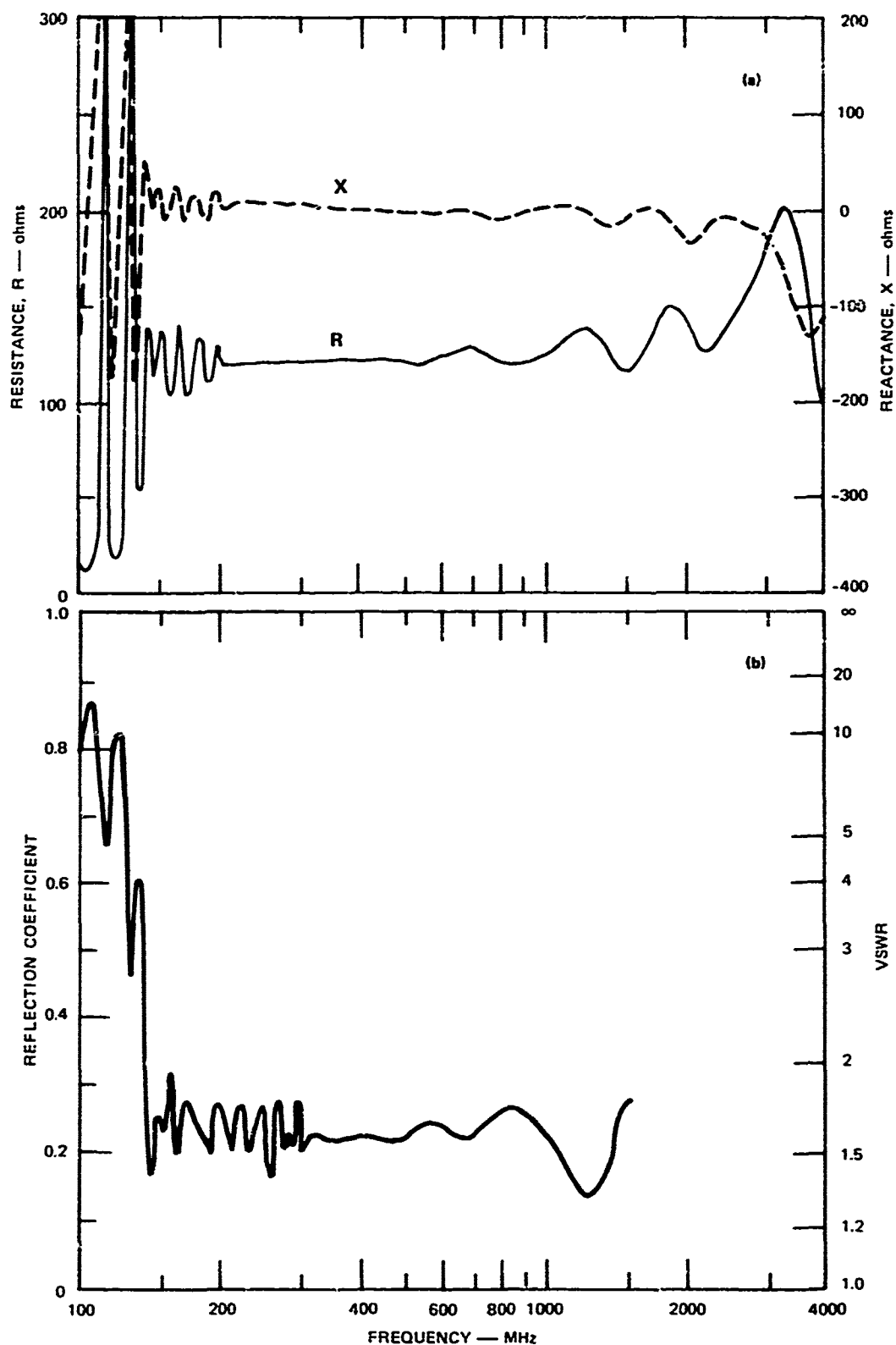
The complex driving-point impedance was measured for the 12-inch and 24-inch spiral antennas when the antennas were placed against

several types of building materials. These materials included (1) a 44-by-46-inch brick and mortar wall, (2) a 44-by-46-inch brick and mortar wall covered with 1/4-inch plaster, (3) a 36-by-48-inch plaster-board (Sheetrock) wall with two studs spaced 8 inches on either side of the center line of the wall (16 inches apart), and (4) a 36-by-48-inch hardwood floor with two joists spaced 8 inches on either side of the center line of the floor (16 inches apart). In each case measurements were taken with the dielectric side of the antenna placed tightly against the center of the material. The antenna was driven by means of the Anzac balun, described in Section II-A, connected to the opposite (metal) side of the antenna. For the wall and floor structures, measurements were also made with the antenna centered over a stud, or joist, and for the latter case the antenna was positioned against the hardwood-floor surface and against the joists supporting the hardwood floor (i.e., underneath the floor). In addition, impedance measurements were obtained with a 30-inch-square sheet of plate glass, 1/16-inch thick, covering the metal side of the antenna and with an oil-painting type canvas between the glass plate and the antenna. For these last measurements, the antenna was supported by styrofoam placed against its dielectric side and was driven by connecting the Anzac balun to the antenna through two small holes cut into the glass and canvas.

D. Driving-Point-Impedance Characteristics of Antennas

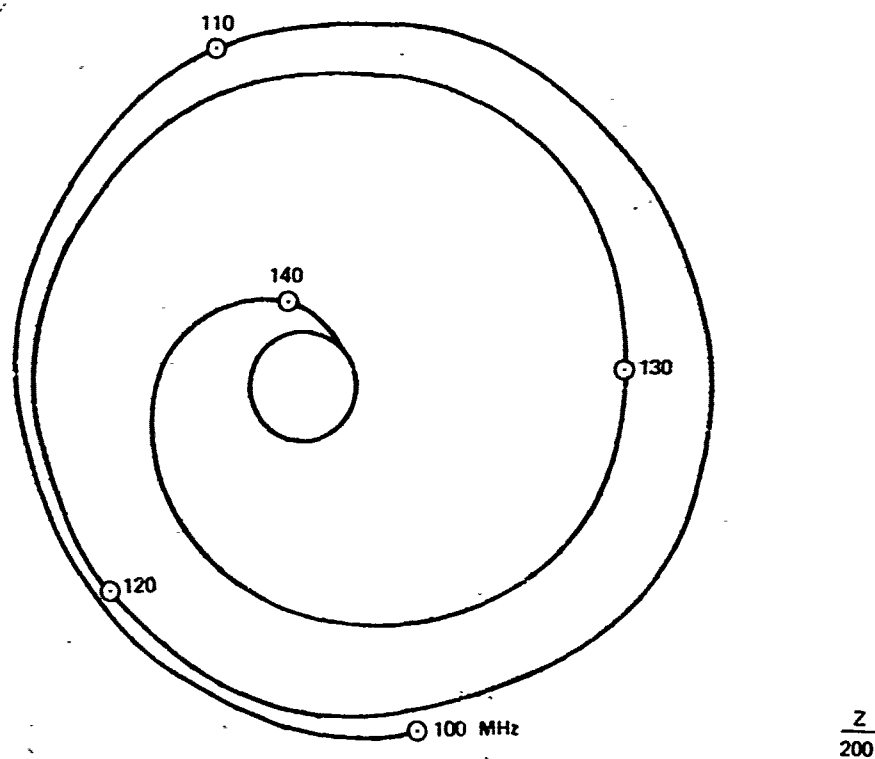
1. Data for the 24-inch Antenna

To establish a reference case, driving-point-impedance measurements were made with the antennas situated in free space. The results for the 24-inch antenna are shown in Figures III-1 and III-2. The real and imaginary parts of driving-point impedance are plotted in Figure III-1(a) as functions of the log of frequency, and the same data are shown on the Smith chart in Figure III-2. The Smith chart is



SA-1370-3

FIGURE III-1 DRIVING-POINT IMPEDANCE AND REFLECTION DATA AT THE CENTER OF THE 24-inch SPIRAL ANTENNA IN FREE SPACE. The reflection data are normalized to 200 ohms (generator impedance). The data were obtained with the outer ends of the spiral left open.



SA-1370-4

FIGURE III-2 SMITH-CHART PLOT FOR 24-inch SPIRAL ANTENNA FED AT THE CENTER WITH A 200-ohm-IMPEDANCE GENERATOR. The outer ends of the spiral were left open. (Frequency range: 100-1500 MHz.)

normalized to 200 ohms, which is the output impedance of the Anzac balun driving the antenna. The Smith-chart plot covers the frequency range from 100 to 1500 MHz, but the impedance plot (Figure III-1(a)) shows additional data obtained at frequencies up to 4000 MHz. These additional data are shown so that the upper frequency limit of the spiral-antenna radiation band can be approximated. Small fluctuations in the driving-point impedance, occurring within the radiating band of the antenna, are caused by reflections from objects in the vicinity of the antenna and to some extent by spiral imperfections. These fluctuations are averaged out of the data presented in Figure III-1 and the subsequent figures of this section. The VSWR and the magnitude of the reflection coefficient are shown in Figure III-1(b). The VSWR would be improved over the radiating frequency band by driving the spiral with a balun whose output impedance was less than 200 ohms.

The radiating frequency band of the spiral antenna may be approximated by determining the frequency range over which the driving-point impedance is relatively constant or over which it exhibits relatively small fluctuations compared to the large fluctuations elsewhere. For the case of the 24-inch antenna in free space, the lower radiating frequency limit, as seen in Figure III-1(a), is about 140 MHz. This frequency is consistent with that measured in the previous contract.¹ The upper radiating frequency limit is somewhat more difficult to determine from Figure III-1(a),* however, but it appears that the antenna will radiate (in the primary mode) well beyond 1500 MHz, which is the specified upper measurement frequency for this contract.

*The accuracy of the impedance curves of Figure III-1 above 2000 MHz is in question because the electrical properties of both the Anzac balun used to drive the antenna and the standard load used in calibration are degraded above this frequency.

Over the radiating frequency range of the 24-inch antenna situated in free space, Figure III-1(a) shows that the real part of the driving-point impedance is about 125 ohms and the imaginary part is close to zero. The driving-point impedance over the radiating frequency range is less than the theoretical value of 188 ohms for self-complementary spiral antennas because the spiral antenna is etched on a dielectric material and because the self-complementary structure of the antenna ends abruptly at the two antenna feed points. The presence of the dielectric material causes the driving-point impedance to decrease because near the center of the antenna the non-radiating fields interact significantly with the dielectric printed circuit board. The non-radiating fields are closely bound within the dielectric material near the antenna center because of the large dielectric-thickness-to-conductor-spacing ratio. The antenna manufacturer, in fact, apparently tried to compensate for the decrease in impedance by departing from the complementary structure along the antenna in the vicinity of its center. The interaction between the non-radiating fields and the dielectric material close to the spiral antenna is discussed in some detail below.

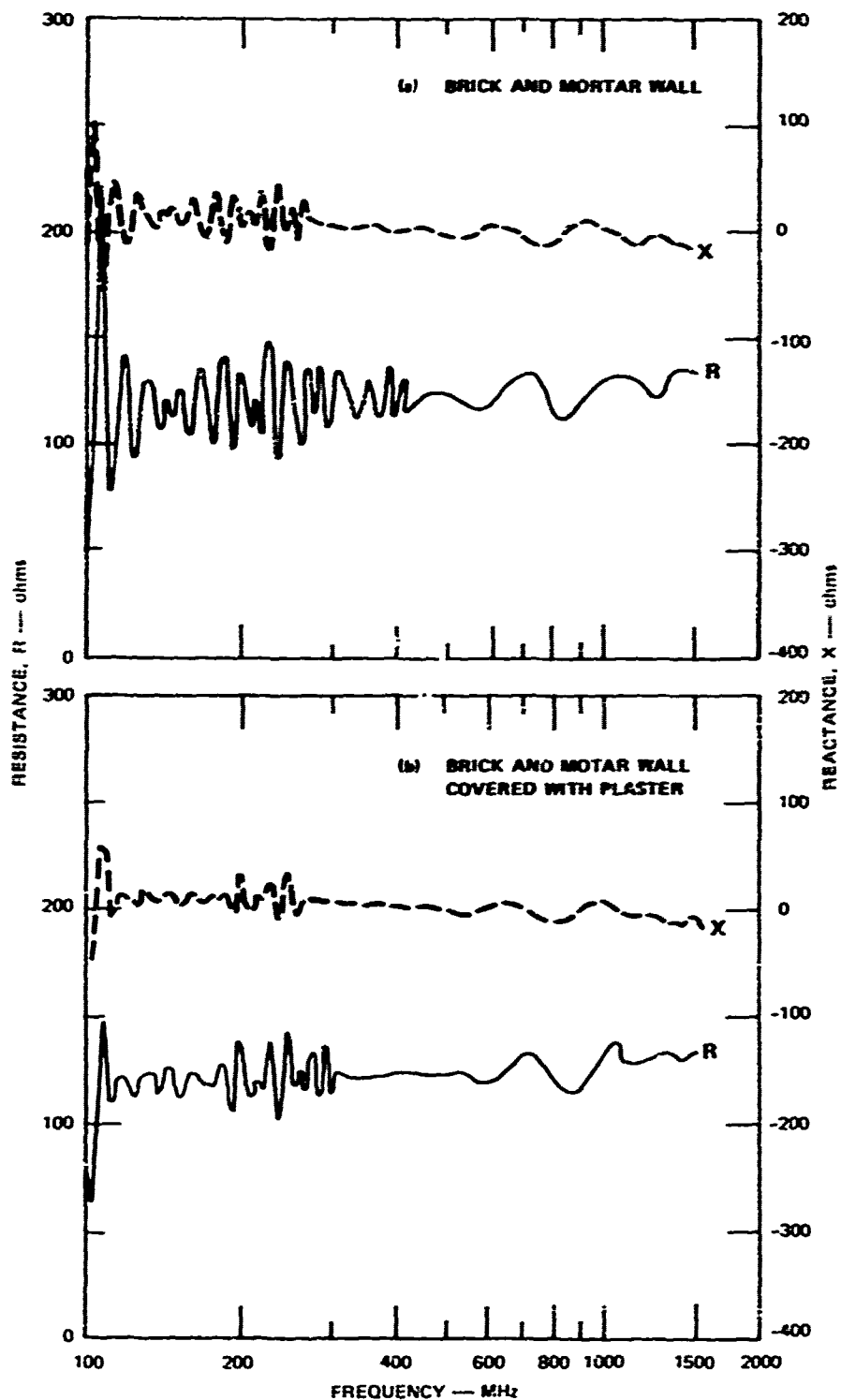
As indicated in Figure III-1, VSWR is nearly constant in the radiating frequency band, but is not near unity. This is because the resistive component of the driving-point impedance is significantly less than 200 ohms and thus a mismatch exists between the spiral antenna and the 200-ohm balun. As seen in Figure III-1, the resistive component averages about 125 ohms in the frequency range between 140 and 1500 MHz. Thus, if the antenna was driven with a 125-ohm balun instead of a 200-ohm balun, the VSWR would improve to a maximum value of 1.12 over the 140-to-1500-MHz frequency range.

Below 140 MHz the 24-inch antenna does not radiate efficiently. Hence, currents reach the ends of the spiral antenna and are reflected

back to the center. This causes the large ripples in driving-point impedance below 140 MHz as seen in Figure III-1. When the data are plotted on a Smith chart, as in Figure III-2, large impedance-curve loops result. As the frequency increases to 140 MHz, the curve spirals inward to a small region. Above 140 MHz, the points fall within the small circle centered at $(0.63 - j0.05)$.

The results of the driving-point-impedance measurements obtained for the 24-inch spiral antenna when in the presence of large dielectric building materials are shown in Figures III-3 and III-4. The relative positions of the antenna and the various dielectric bodies are described in Section III-C. In both figures the real and imaginary parts of driving-point impedance are plotted as functions of the log of frequency. It was indicated previously that only the driving-point impedance within the radiating frequency band of the spiral antennas is of interest; hence, the following discussion concentrates on the data obtained within this frequency band.

It is noted, first of all, that the radiating frequency band changes depending on the type of dielectric material placed against the antenna. This is seen when comparing Figures III-3 and III-4 with Figure III-1, which shows the driving-point-impedance data for the case when no dielectric building materials are pressed against the antenna. Specifically, the lower radiating frequency limit is less for the cases where building materials are positioned against the antenna than it is for the case when the antenna is situated away from all building materials. This is because the radiating fields interact with the added dielectric material at the outer ends of the spiral, resulting in a decrease of the wavelength on the spiral. This is discussed further in Section III-D-2 below.



SA-1370-5(a)

FIGURE III-3 DRIVING-POINT IMPEDANCE OF THE 24-inch SPIRAL ANTENNA PLACED IN JUXTAPOSITION WITH SEVERAL TYPES OF DIELECTRIC BUILDING MATERIALS. The measurements were taken with the dielectric side of the antenna against the material and with the outer ends of the spiral left open.

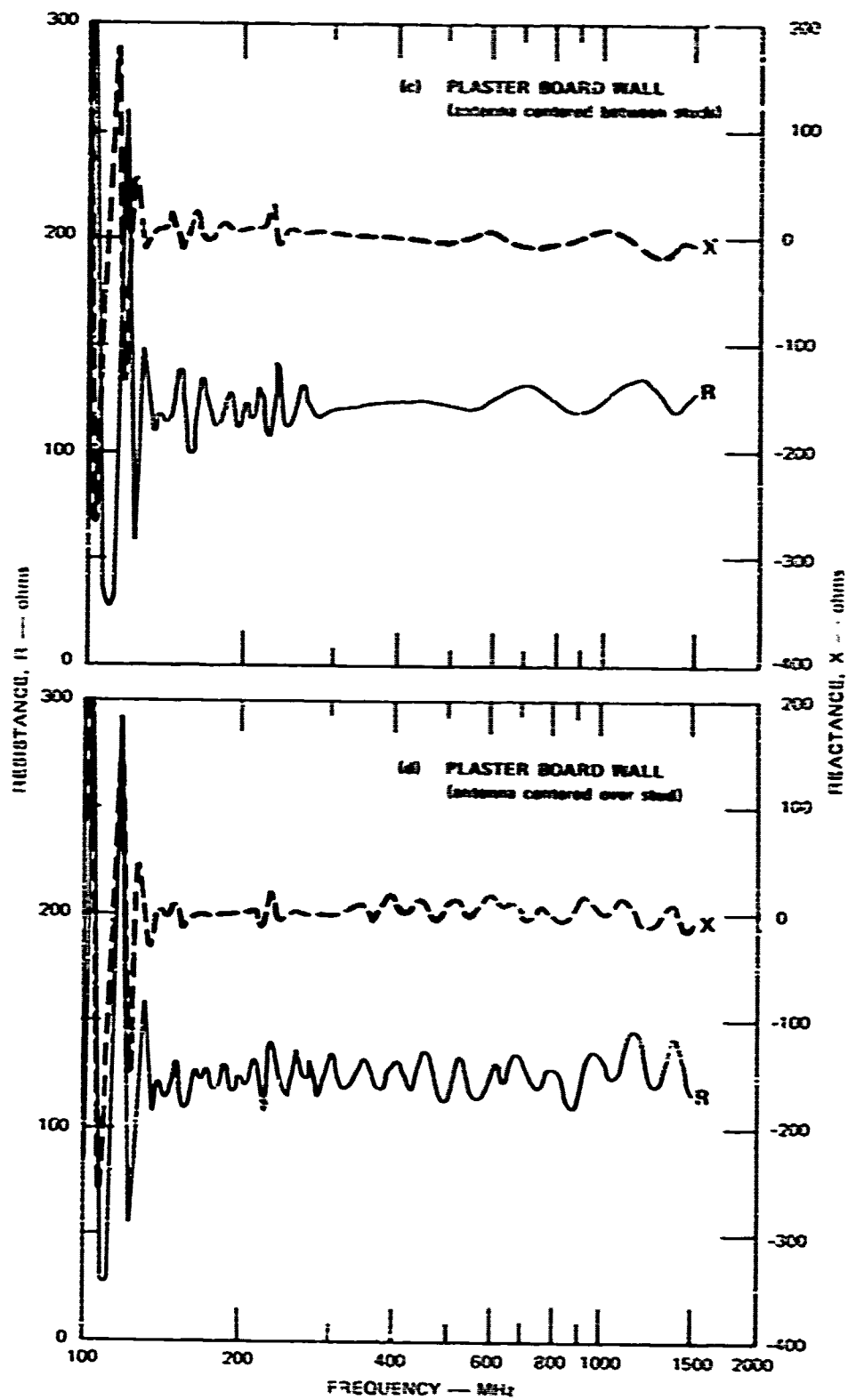


FIGURE III-3 (Continued)

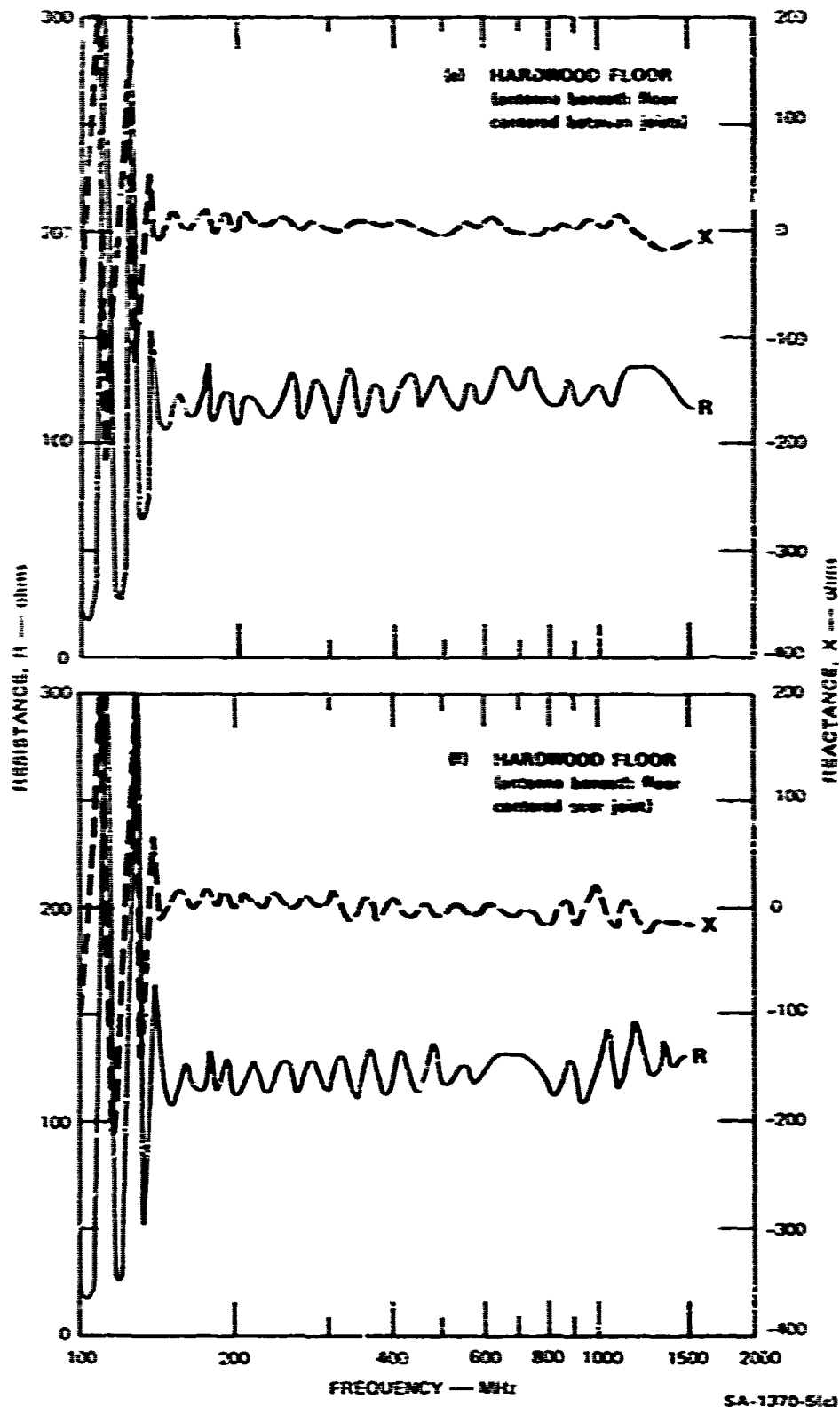


FIGURE 11-3 (Continued)

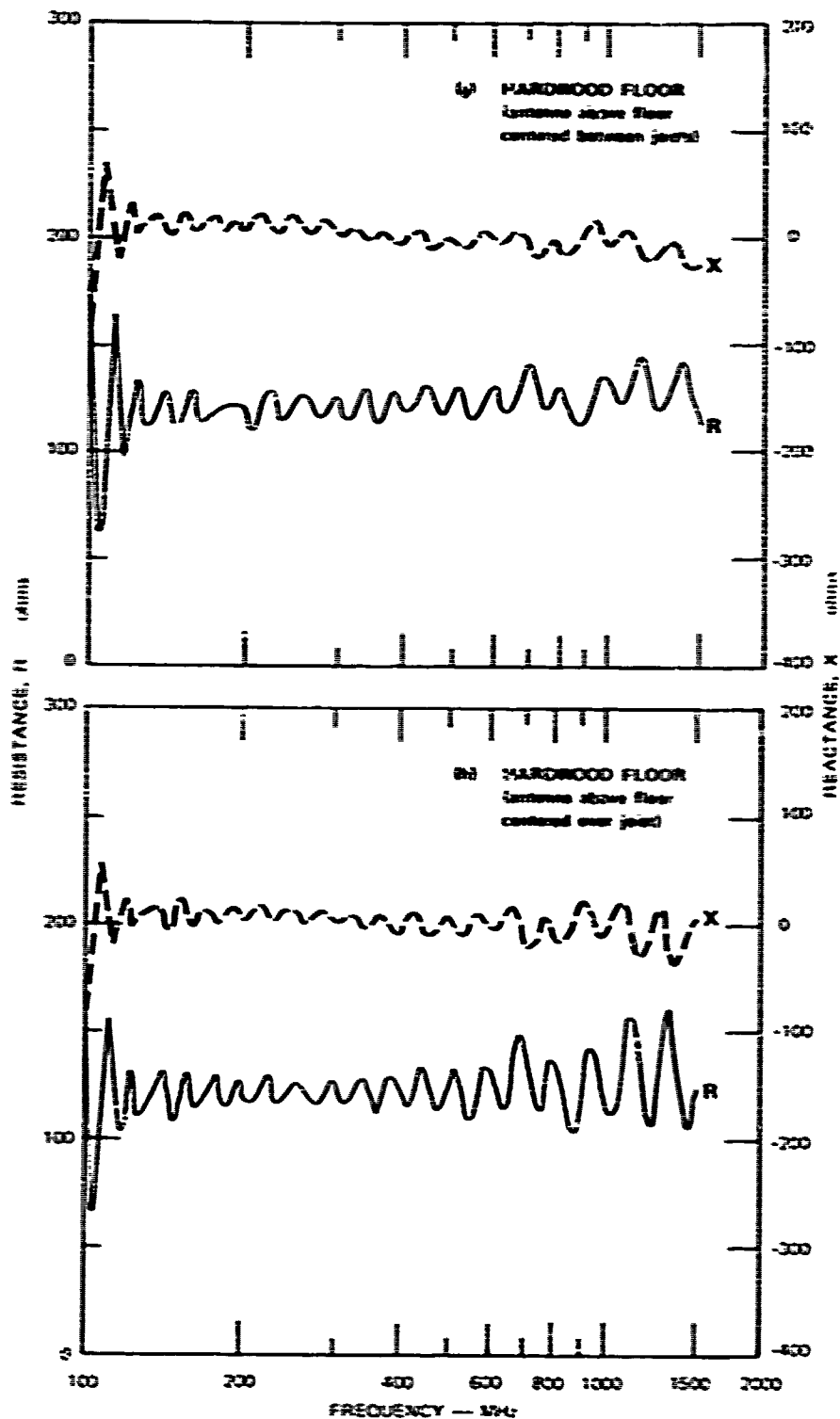


FIGURE III-3 (Concluded)

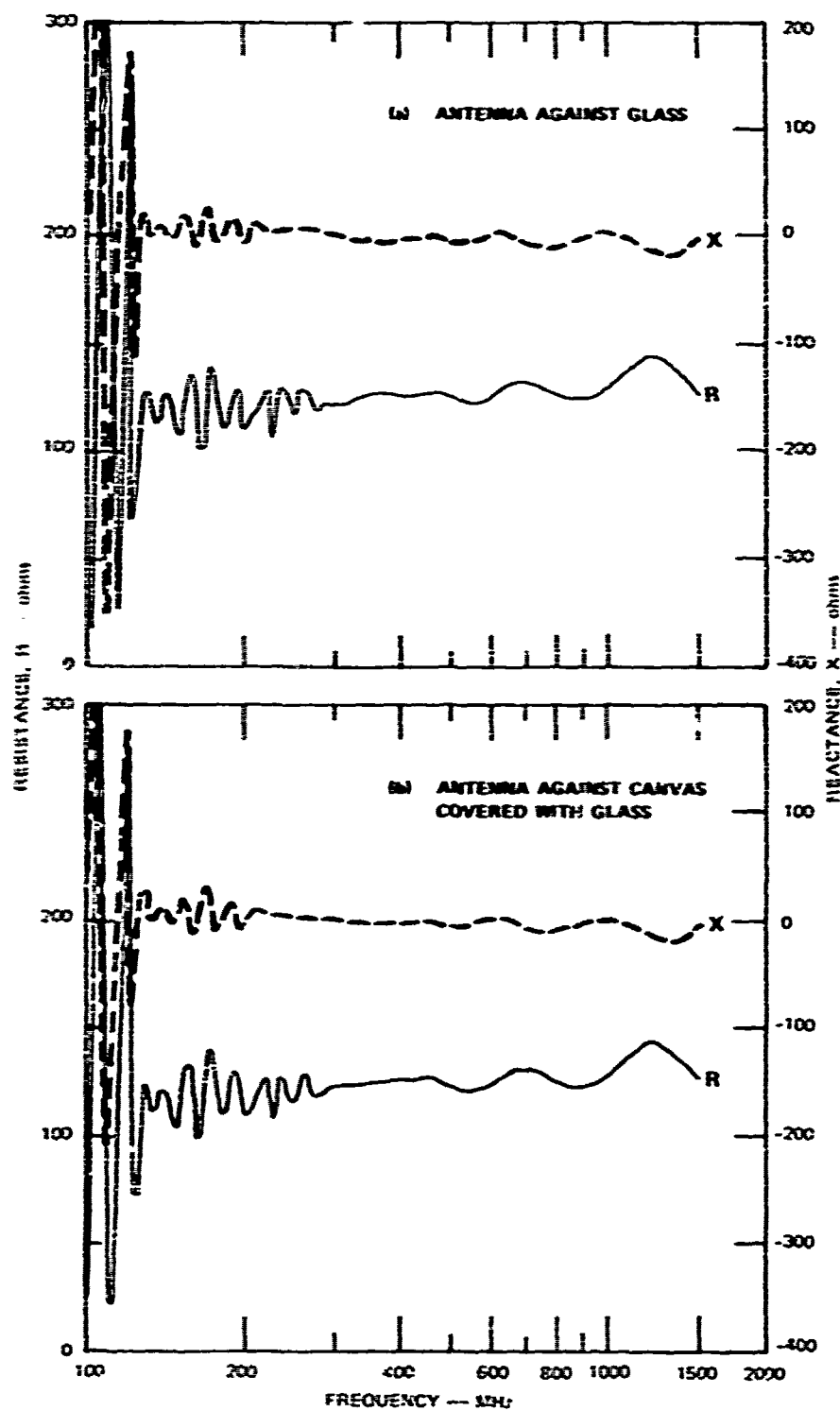


FIGURE III-4 DRIVING-POINT IMPEDANCE OF THE 24-inch SPIRAL ANTENNA PLACED AGAINST GLASS AND CANVAS. The measurements were taken with the metal side of the antenna against the glass and the glass covering both canvas and antenna. The antenna was supported in free space by a styrofoam backing and the outer ends of the spiral were left open.

As seen in Figures III-3 and III-4, some driving-point-impedance fluctuations exist within the radiating frequency band of the 24-inch antenna placed in juxtaposition with the building materials. These fluctuations are caused by multiple reflections from the dielectric material inhomogeneities and from foreign objects within the material such as nails. The fluctuations caused by multiple reflections from objects such as nails [Figures III-3(d) and III-3(e), for example] are approximately periodic with the log of frequency. This is because the nails interact mostly with the radiating fields but interact only slightly with the non-radiating fields. That is, the input wave travels the length of the spiral from the feed to the radiating regions, and some of the wave is reflected from the nails and travels back along the spiral to the feed. The feed-to-radiating-region path length is inversely proportional to the ratio of the input frequency to some reference frequency. That is, the path length is proportional to minus the logarithm of frequency. Below the radiating frequency band the fluctuations are periodic with frequency (and hence appear aperiodic on the semilog plots of Figure III-3^{*}) because reflections take place at fixed points on the spiral (i.e., at the outer ends of the spiral). The fluctuations within the radiating frequency band, however, are considerably less in amplitude than the impedance fluctuations outside the radiating frequency range that are caused by reflections from the ends of the spiral antenna. Most significantly, though, is the fact that over the radiating frequency range of each antenna/building-material combination, the average driving-point impedance is essentially the same and furthermore differs insignificantly from the driving-point impedance of 125 ohms for the 24-inch antenna situated in free space (Figure III-1).

* This is more evident on the 12-inch antenna plots of Figure III-7.

Figure III-4 shows the driving-point impedance of the antenna for two cases when glass was placed against the metal side of the antenna. Once again, the driving-point impedance is about the same as for the antenna in free space.

In summary, the impedance data of Figures III-1 through III-4 show that, on the average, the driving-point impedance of the 24-inch spiral antenna is 125 ohms over the radiating frequency band of the antenna and is unaffected by the presence of the various types of building materials brought in contact with the antenna. This is true as long as the fields excited by the antenna near its center do not interact with the building material. For the situations represented in Figures III-1 through III-4, negligible interaction of these fields with the various building materials occurred. In one case the materials were separated from the metal spiral by the antenna dielectric support; in the other case the spiral and glass (or canvas) dielectric were separated by air. The result that driving-point impedance is virtually constant under the various conditions described above is desirable, for it means that one matching network will suffice to match a 50-ohm source impedance to the antenna driving-point impedance for all these conditions.

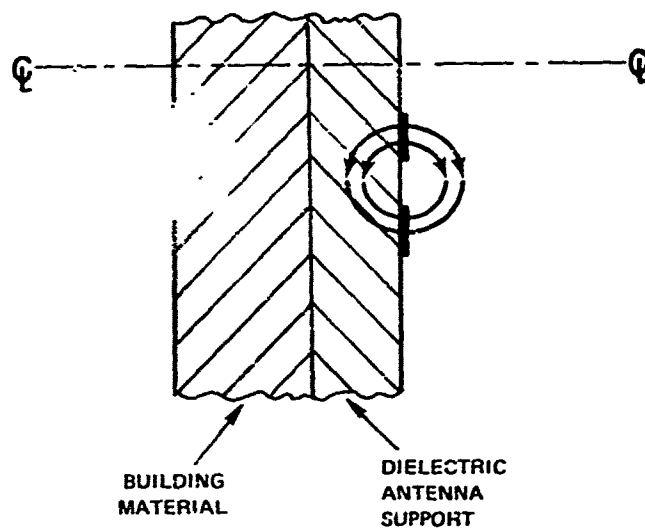
2. Discussion of Characteristics

a. Impedance

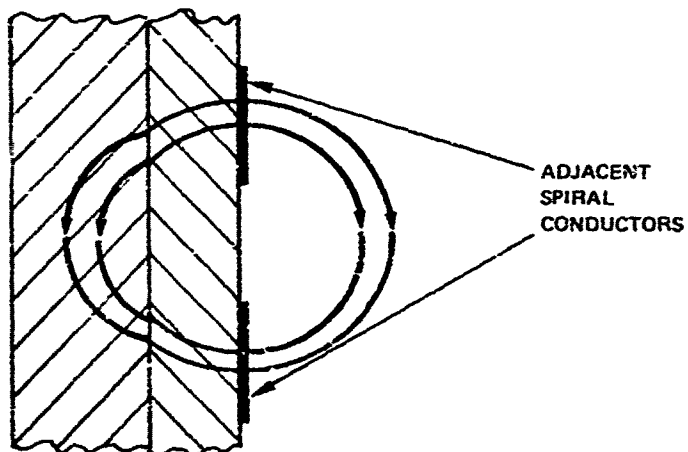
The reason that the driving-point impedance over the radiating frequency band of the antenna is essentially unaffected when the antenna is placed against large dielectric bodies can be explained using the transmission-line analogy introduced in Section III-B-2. As mentioned there, the spiral antenna can be thought of as consisting of two regions. These are the non-radiating region in the center of the antenna, and the radiating region. There is, of course, a gradual

rather than a sharp transition between the two regions. Other non-radiating and radiating regions also exist outside the primary radiating region, but are of no interest here. The fields and modes that exist in these two different regions are very different from each other. The exact details of the currents and fields in the two regions need not be known, however, for the following qualitative discussions in this subsection and Section III-D-2-b.

Consider first how the dielectric sheet supporting the spiral conductors affects the characteristic impedance of the equivalent-transmission-line representation of the non-radiating region. Near the antenna center, where all dimensions are very small compared to wavelength, the currents flowing along the spirals will be nearly out of phase in adjacent conductors. Most of the electric fields that start on one conductor can be expected to terminate on the adjacent conductors, and thus will not extend far from the plane containing the spirals. The situation will be somewhat analogous to the two-strip transmission lines shown in cross section in Figure III-5. In Figure III-5(a), the spacing between strips is small compared to the thickness of the support dielectric, so that most of the electric field on the dielectric side of the strips is within the dielectric. The result on impedance is essentially the same as if the support dielectric were infinitely thick. Adding a second dielectric on the same side, then, such as the building material indicated in Figure III-5, will not change the impedance of the transmission line significantly. This situation is analogous to that existing at the center of the spiral antenna. For the strips shown in Figure III-5(b), on the other hand, the strip spacing is not small compared to the thickness of the support dielectric, and much of the electric field passes through it. The characteristic impedance of this widely spaced transmission line will be affected by the absence or presence of additional dielectric beyond the support dielectric.



(a) NEAR ANTENNA CENTER



(b) FAR FROM ANTENNA CENTER

SA-1370-9

FIGURE III-5 CROSS-SECTION VIEW OF SPIRAL ANTENNA DEPICTING INTERACTION OF NON-RADIATING FIELDS WITH DIELECTRIC BUILDING MATERIAL BROUGHT IN CLOSE CONTACT WITH ANTENNA

This situation is analogous to a part of the spiral antenna far from the antenna center yet still in the non-radiating region.

The usual printed spiral antennas are proportioned such that the ratio of spiral width to spacing to the next spiral is the same at any location on the antenna. If these conductors are in a uniform dielectric medium, such as free space, then the impedance level seen by a non-radiating wave traveling along the spirals will be the same at all positions on the spiral. The conductors of the antennas being discussed are not in free space, but are supported on a dielectric sheet of uniform thickness. The ratio of this dielectric thickness to spacing between adjacent conductors is large at the antenna center, but small at the outside edge. As a result, the equivalent impedance seen by a non-radiating wave will be a function of position along the spiral. The impedance will vary from low at the input terminals to a higher value approaching the impedance of the spiral in free space as the wave propagates outward along the spiral.*

* Some numerical values might be of interest even though they are not essential to the discussion. For a self-complementary, zero-thickness spiral in free space, the theoretical input impedance is 188 ohms. If such a spiral were mounted on an infinitely thick piece of dielectric with relative dielectric constant, ϵ_r , it is expected that the impedance would be lowered to $188/\sqrt{(1 + \epsilon_r)/2} = 109$ ohms for $\epsilon_r = 5$. An $\epsilon_r = 5$ is typical of epoxy-fiberglass circuit boards, but is not known to apply to these antennas. Thus, an impedance level on the order of 110 ohms could be expected at the antenna center. Two other factors also influence the impedance. One is that the ratio of conductor thickness to conductor spacing is great enough near the antenna center to further lower the impedance. The second factor is that these antennas are constructed with the spiral width near the antenna center less than that of a self-complementary structure, which raises the impedance to partially compensate for the impedance-lowering factors.

The impedance taper along the spiral is not necessarily undesirable. The impedance changes slowly along the spiral, so the input wave experiences only small reflections as it propagates along the taper. Once the wave reaches the radiating region most of the power is radiated, still with essentially no reflection. As long as none, or very little, of the input wave is reflected back toward the driving generator, the input impedance is constant and equal to the characteristic impedance at the input of the spiral.

Based on the preceding discussion, it is now obvious why the measured driving-point impedance does not change significantly when the spiral antenna is placed with its dielectric side against various dielectric building materials. The building material lowers the impedance for those portions of the spiral far from the center, but not at the center. The impedance taper along the spiral is changed, but it is still a gradual taper with low reflection. Therefore, the input impedance is still equal to the same spiral-center characteristic impedance.

The particular case where the glass was placed on the metal side of the antenna requires separate comment. It was discovered after the data were taken that the metal eyelets forming the connections to the spiral center held the glass away from the spiral conductors. The resulting air gap was evidently thick enough that the closely bound non-radiating fields did not extend from the spiral out to the glass at the antenna center. In this case again, the material close to the antenna did not change the impedance at the antenna center. It did, of course, interact with the fields farther out on the antenna to cause a new, but gradual and reflectionless, impedance taper with the same input impedance.

Thus it is seen that the impedance taper is not only innocuous, but the presence of the dielectric that causes the impedance

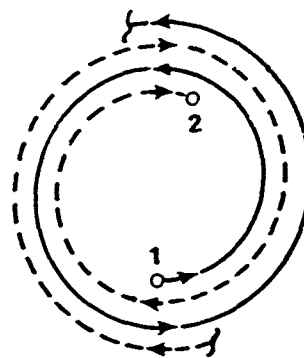
taper has an unexpected benefit. This benefit is that the antenna driving-point impedance is very insensitive to the presence of other dielectric materials near the antenna.

b. Cutoff Frequencies

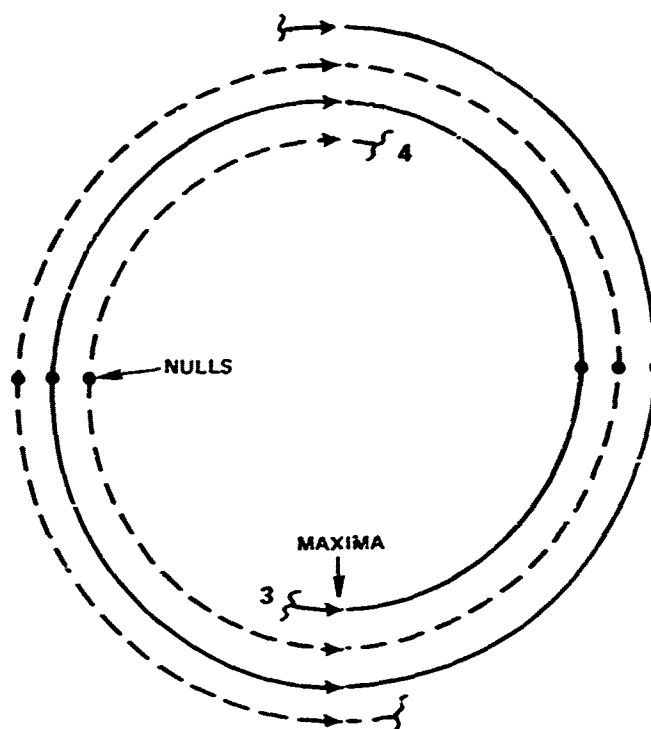
As has been stated earlier in the report, the radiation cutoff frequencies are determined by the one-wavelength-circumference radiation region touching the outer or inner ends of the spiral. In order to explain how the presence of dielectric materials near the spiral affects the cutoff frequencies, it will be helpful to review why some regions of the antenna do not radiate but others do radiate. For simplicity, the discussion will begin assuming no dielectric near the spiral conductors.

Figure III-6(a) shows some turns of the spirals in a region where all dimensions are very small compared to wavelength. For simplicity, only thin lines are used to indicate the spirals. Consider some instant in time when current is flowing onto the solid-line spiral at Point 1; and off of the other spiral at Point 2 as indicated by the arrows. Following the solid-line spiral around a half turn, a full turn, etc., the current has undergone negligible phase shift, so it is still oriented counterclockwise. Similarly, all current arrows on the dashed-line spiral are oriented clockwise.* Both currents are continuous along the conductors, even though only discrete arrows appear on the figure. Note the alternating directions of the current arrows. The far-field radiation component from any given current increment is canceled by the opposite current in the adjacent conductor. Not only that, but the

*The reader is reminded that this discussion is only qualitative. See Ref. 8 for fine details of the actual current distributions.



(a) FEED REGION,
RADIUS $\ll \lambda$



(b) RADIATION REGION,
AVERAGE RADIUS = $\lambda/2\pi$

SA-1370-10

FIGURE III-6 CURRENT RELATIONSHIPS ON A SPIRAL ANTENNA

current on the same conductor is oppositely directed in space a half turn around the spiral.

Now consider a region that is not small compared to wavelength--specifically, the region with average circumference equal to a wavelength. At some time instant, a current maximum exists with the current direction counterclockwise at Point 3 on Figure III-6(b). Recalling that the current for a traveling wave varies sinusoidally along the direction of propagation, it is clear that at the given time instant the current is zero a quarter turn around the spiral, and maximum again a half turn around the spiral. The current at this second maximum is, however, reversed from counterclockwise to clockwise. Note that both current arrows now point to the right, so that their contributions to the far-field radiation along the antenna axis add in phase. Point 4 in Figure III-6(b) is on the other spiral and is chosen to be the same distance from the feed as Point 3. Thus the currents at Points 3 and 4 are still out of phase in the sense of direction of travel along the spirals. Compare the arrow orientations at Points 1 and 3 and at Points 2 and 4. The current at Point 4 is clockwise, and reverses to counterclockwise a half turn around the dashed-line spiral. Now the current increments in adjacent conductors are in the same direction as seen from a distant point on the antenna axis, so that all radiation components add in phase. *

For a few turns of the spirals inside and outside the wavelength-circumference circle, the current maxima will depart from the

* At this time instant, all the currents pictured in Figure III-6 are radiating a linearly polarized field. As time progresses, the currents turn as they follow the spiral. The result is that the far-field vector rotates once per RF cycle--that is, the far field is circularly polarized.

half-turn spacing depicted in Figure III-6(b), and the current increments spaced around the spiral a half turn will depart somewhat from radiating exactly in phase. The phase relationships are close enough to being correct, however, that significant radiation occurs from several turns. Just how many turns depends on how tightly the spiral is wound.

Now that the necessary phase relationships for good radiation have been covered, the effect of adding dielectric material near the spiral conductors will be discussed. Obviously, mounting the spirals on a dielectric support sheet will slow the wave as it propagates out along the conductors. For a given excitation frequency, then, the wavelength along the spiral will be shortened, and the diameter of the radiating region decreased. Referring to Figure III-5, it is readily apparent that the wave will be slowed the most near the antenna center where the electric fields to the left of the spiral are all within the support dielectric, and the wave will be slowed very little out near the antenna edge where most of the electric field on the left passes through the support dielectric and out into air again. Thus it is expected that the dielectric support sheet will lower the upper cutoff frequency for the primary radiation mode considerably,* but the dielectric support sheet will lower the lower cutoff frequency only slightly.

Finally, when the antenna is placed with its dielectric side against the building materials, the fields near the spiral center

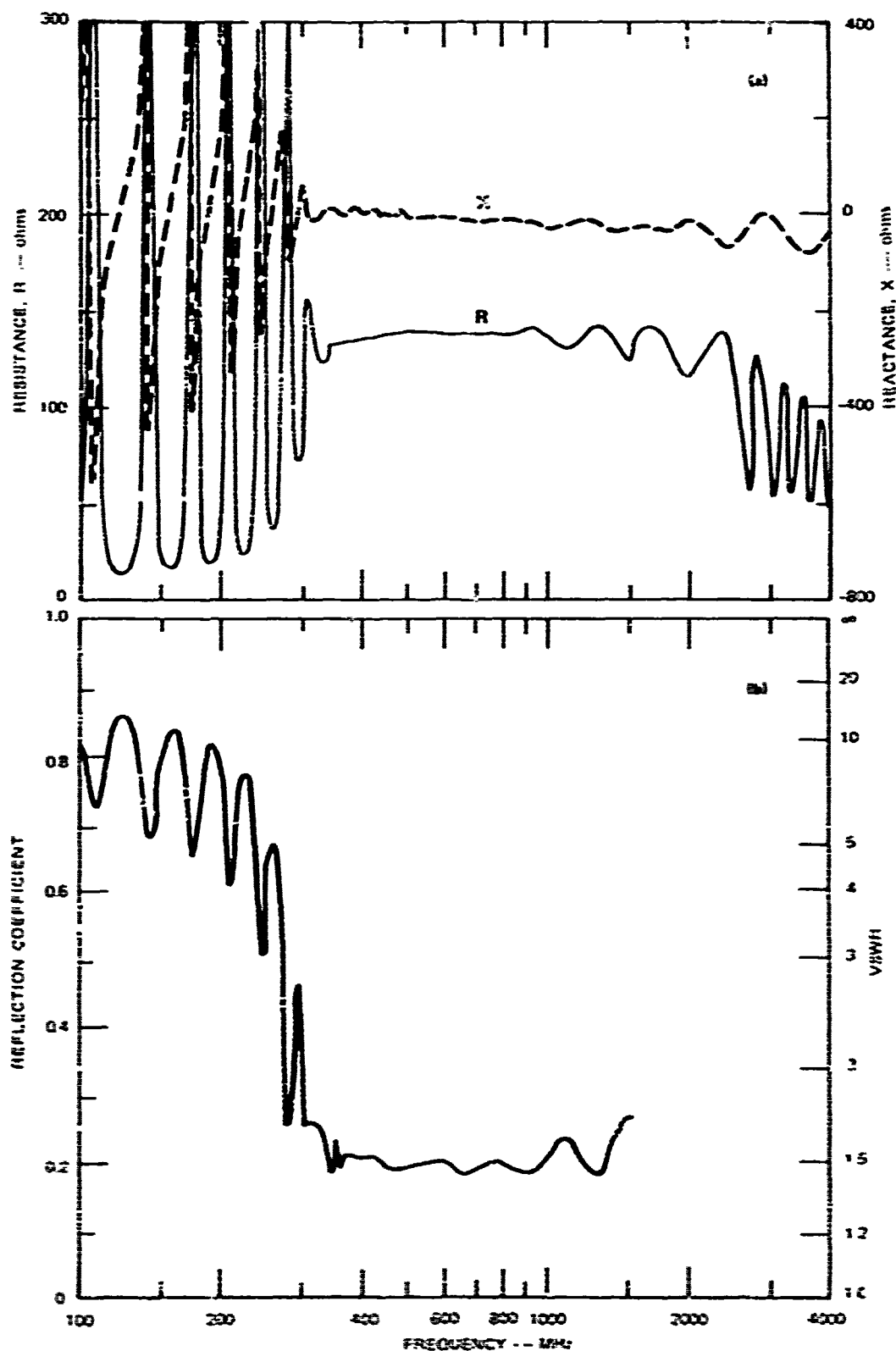
* An estimate of the change factor for the upper cutoff frequency is $1/\sqrt{\epsilon_r + 1}/2 \approx 0.6$ (i.e., -40 percent change), for a support dielectric constant $\epsilon_r = 5$.

do not reach that material, so the upper cutoff frequency is not lowered further. The fields near the outside of the antenna do extend into the building material as illustrated in Figure III-5(b), so that the presence of the additional dielectric will lower further the lower radiation cutoff frequency. The data of Figures III-1 through III-4 clearly show this effect.

3. Data for the 12-Inch Antenna

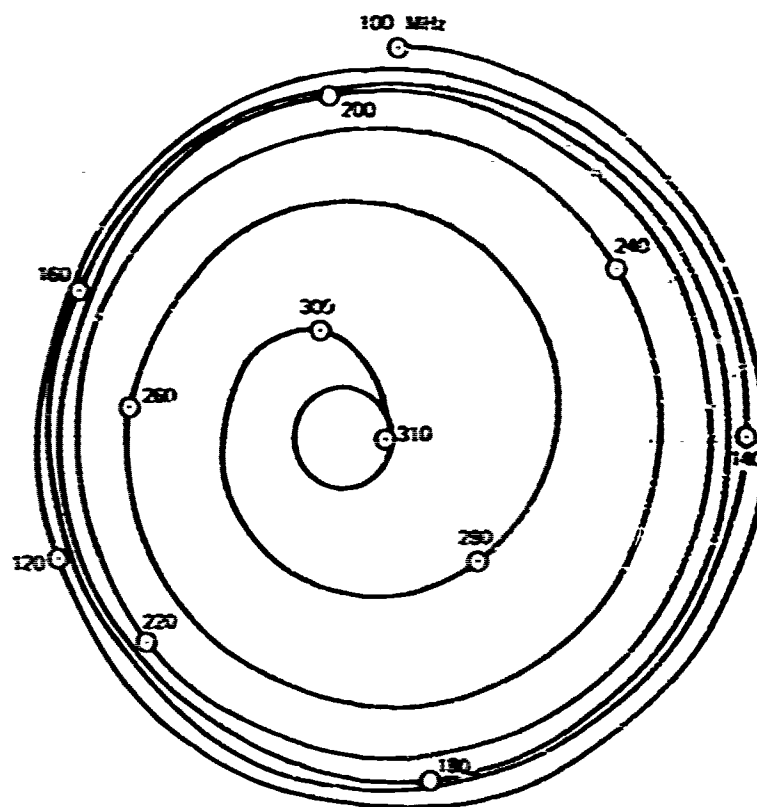
The measured driving-point impedance and related data for the 12-inch spiral antenna are shown in Figures III-7 through III-9. The real and imaginary parts of driving-point impedance are plotted in Figure III-7(a) as functions of the log of frequency for the case when the 12-inch antenna is situated in free space; the same data are shown on the Smith chart in Figure III-8. As in the case of the 24-inch-antenna measurements, the Smith chart is normalized to the 200-ohm Anzac balun output impedance, and the plot covers the frequency range from 100 to 1500 MHz. The VSWR and the magnitude of the reflection coefficient are shown in Figure III-7(b). The real and imaginary parts of driving-point impedance are plotted as functions of the log of frequency in Figure III-9 for several of the 12-inch-antenna building-material combinations discussed in Section III-C.

The 12-inch spiral antenna is essentially a 2:1 scaled-down version of the 24-inch antenna. Two parameters that are not scaled, however, are the thickness of the dielectric circuit board supporting the antennas and the thickness of the spiral stripline conductors. The thickness of each is the same for both antennas--nominally 0.060 inch for the dielectric and 0.0028 inch for the conductors. Because of these two discrepancies in scaling, both the driving-point impedance characteristics and the 2:1 frequency-scaling factor are affected somewhat.



52-1370-11

FIGURE III-7 DRIVING-POINT IMPEDANCE AND REFLECTION DATA AT THE CENTER OF THE 12-INCH SPIRAL ANTENNA IN FREE SPACE. The reflection data are normalized to 200 ohm (generator impedance). The data were obtained with the outer ends of the spiral shorted to the antenna supporting ring.



$\frac{Z}{200}$

SA-1120-12

FIGURE III-5 SMITH-CHART PLOT FOR 12-INCH SPIRAL ANTENNA FED AT THE CENTER WITH A 200-ohm IMPEDANCE GENERATOR. The outer ends of the spiral are shorted to the antenna supporting ring. (Frequency range: 100-1500 MHz.)

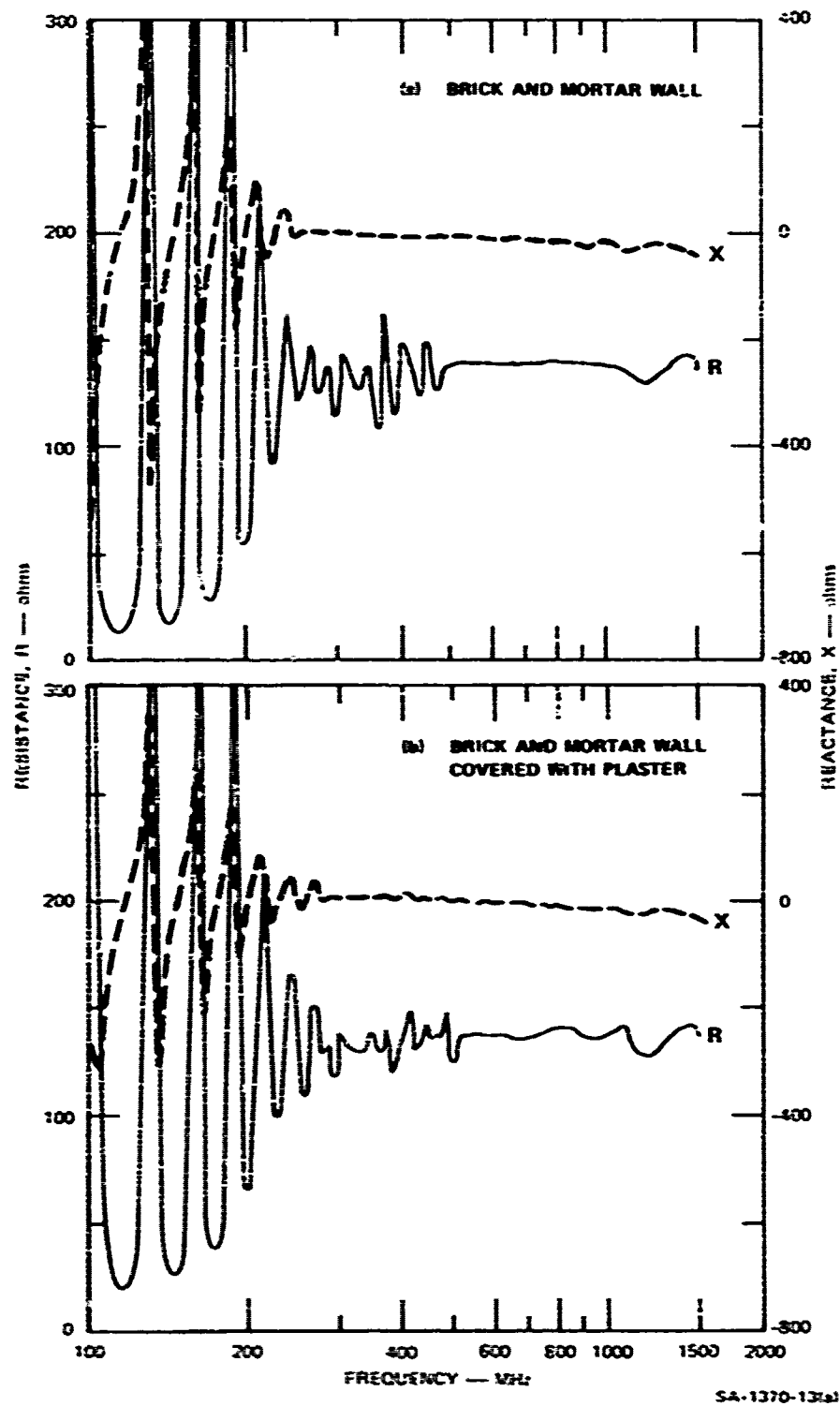


FIGURE III-9 DRIVING-POINT IMPEACANCE OF THE 12-inch SPIRAL ANTENNA PLACED IN JUXTAPOSITION WITH SEVERAL TYPES OF DIELECTRIC BUILDING MATERIALS. The measurements were taken with the dielectric side of the antenna against the material and with the outer ends of the spiral shorted to the antenna supporting ring.

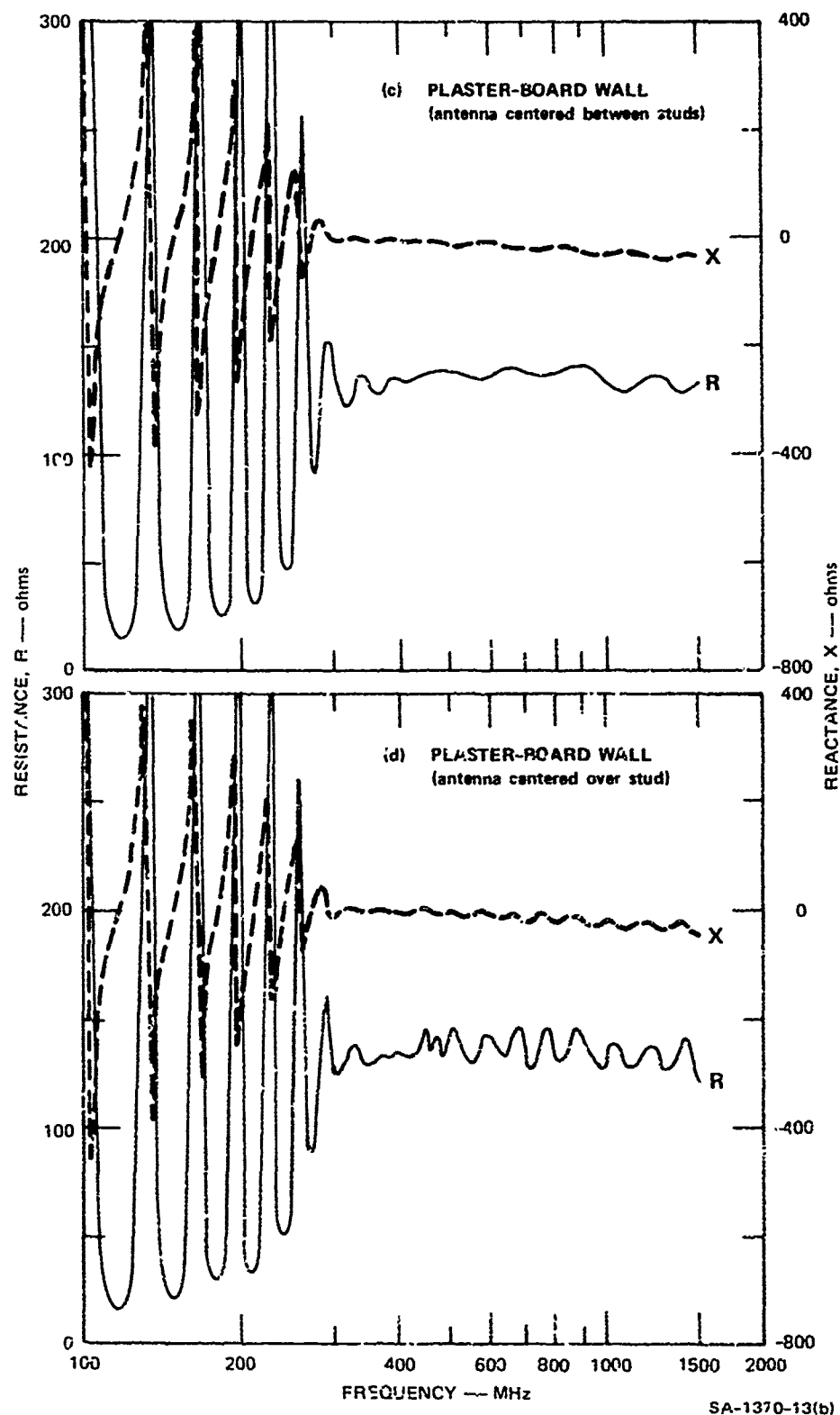


FIGURE III-9 (Continued)

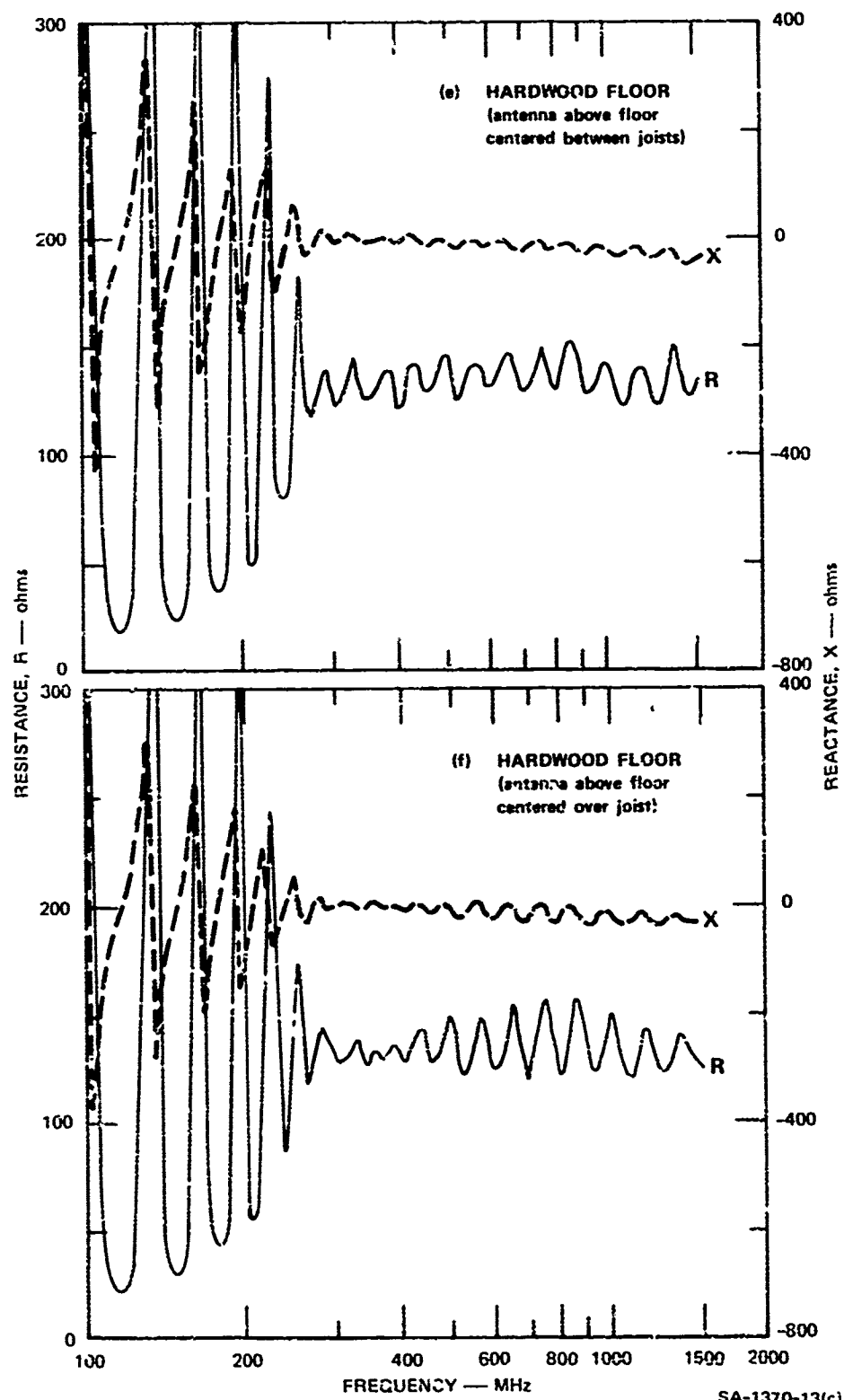


FIGURE III-9 (Concluded)

This is seen when comparing the 12-inch-antenna impedance data with the 24-inch-antenna impedance data. Figure III-7(a) shows, for example, that the average driving-point impedance over the radiating frequency range of the 12-inch antenna is about 137 ohms. The radiating frequency range is seen to begin at about 300 MHz and to extend beyond the 1500-MHz upper-operating-frequency requirement. These values are for the case when the 12-inch antenna was situated in free space. Comparable values for the 24-inch antenna, as seen from Figure III-1(a), are 125 ohms for the average driving-point impedance and 140 MHz for the lower-radiating-frequency limit. The driving-point impedances are not exactly equal because the important ratios of the spiral conductor dimensions (thickness, width, and the spiral complementary spacing) to the thickness of the dielectric circuit board supporting the antenna are not maintained equal for the two antennas. For this reason also, the frequency scaling is not exactly 2:1; hence, the lower radiating frequency limit of the 12-inch antenna is not exactly twice that of the 24-inch antenna as one might expect, since the circumferences of the two antennas differ by a factor of two.

The data plotted in Figures III-7(b) and III-8 are essentially the same data shown in Figure III-7(a) but in different form. Figure III-7(b) shows the reflection coefficient and VSWR, as functions of the log of frequency, looking into the feed terminals relative to a 200-ohm source impedance. If the antenna was driven by a 137-ohm source, the VSWR would improve to a maximum value of 1.13 over the 300-to-1500-MHz frequency band. The Smith-chart data (Figure III-8), which also are relative to 200 ohms, show large impedance-curve loops occurring outside the radiating frequency band. As discussed previously for the 24-inch antenna Smith-chart plot, the large loops are due to the long path length that the energy reflected from the outer ends of the spiral must travel. As the frequency increases to 300 MHz, the curve spirals

inward to a small region. Above 300 MHz the points fall within the small circle centered at $(0.68 + j0)$.

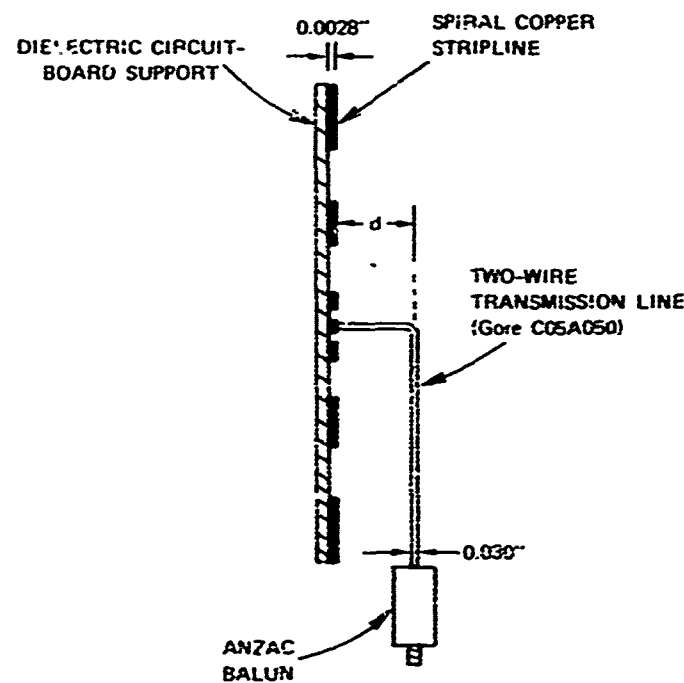
The data plotted in Figure III-9 show the driving-point-impedance characteristics of the 12-inch antenna when in the presence of various dielectric building materials that were discussed in Section III-C. As for the case of the 24-inch antenna, the building materials were brought against the dielectric support side of the antenna. The impedance data of Figure III-9 are comparable to the impedance data for the 24-inch antenna shown in Figure III-3. The differences between the data are the same discussed above: The 2:1 frequency scaling is not exact, nor are the driving-point impedances measured under the same conditions exactly equal. As before, the driving-point impedance within the radiating frequency band of the antenna fluctuates with frequency, but on the average equals the value of impedance when the antenna is situated in free space (Figure III-7). The reason the presence of the dielectric materials does not affect the driving-point impedance within the radiating-frequency range of the antenna has been previously discussed in connection with the 24-inch-antenna data, and no further discussion will ensue here. Let it suffice to say that the average driving-point impedance measured for the 12-inch spiral antenna within the radiating frequency band is 137 ohms, and, as for the case of the 24-inch antenna, remains the same for all the conditions under which the measurements were made.

IV DRIVING-POINT IMPEDANCE OF A SPIRAL ANTENNA FED BY A TWO-WIRE TRANSMISSION LINE

The purpose of this section is to show how the driving-point impedance of a spiral antenna is affected by running a two-wire transmission line in close proximity to the antenna. The effect on driving-point impedance due to the presence of a transmission line is of concern because of the low-profile requirement on the antenna and associated matching-network configuration. This requirement necessitates moving the matching network (the compact balun discussed in Section V) from the center to the edge of the antenna and connecting the two by means of a two-wire transmission line.

The 12-inch spiral antenna was used in this investigation. The antenna was driven by the 200-ohm Anz c balun (see Section II-A) that was connected to the antenna by means of twin-lead-parallel-pair transmission line, ^{*} 19.3 cm long. The transmission line first extended perpendicularly from the antenna feed terminals and then turned to run parallel with the copper printed-circuit side of the antenna as shown in Figure IV-1. The orientation of the transmission line was such that the plane containing its two wire conductors was parallel with the plane of the antenna. The transmission line was turned parallel with the antenna in this plane, with a small radius bend as opposed to a sharp right-angle bend. Driving-point-impedance measurements were made for various values of d indicated in Figure IV-1. The distance, d , in this figure is defined as the distance from the spiral conductors to the plane containing the wire centers for the two-wire transmission line.

* Gore and Associates, C05A050.



SA-1070-6

FIGURE IV-1 CROSS-SECTION VIEW OF ANTENNA/TRANSMISSION-LINE-FEED CONFIGURATION

The driving-point impedance for the various positions of the transmission line was found by measuring the complex reflection coefficient at the connection between the balun and transmission line and mathematically determining the impedance at the antenna-feed terminals. To do this it was necessary to know the characteristic impedance and electrical length of the transmission line. Both parameters were measured with the network analyzer (see Section II-A). The characteristic impedance was found to be 159.2 ohms^{*} and the electrical length for the 19.3-cm line was found to be 28 cm. The measured reflection data, normalized to the 300-ohm balun output impedance, was renormalized to the characteristic impedance of 159.2 ohms. The data reference

^{*}The manufacturer specified the characteristic impedance of the transmission line (Gore CC5A050) to be 150 ohms.

plane at the connection between the balun and transmission line was shifted 28 cm along the electrical length of the transmission line to the antenna-feed terminals. With this plane used as the reference, the driving-point impedance of the antenna was then determined from the renormalized reflection coefficient data. The assumption was made that the transmission-line losses were negligible.

The real and imaginary parts of driving-point impedance over the frequency range from 100 to 1500 MHz are plotted in Figure IV-2 for various values of distance, d , defined in Figure IV-1. The figure shows that when the transmission line is close to the antenna, there is significant fluctuation of driving-point impedance with frequency in the radiating band of the antenna.* When the transmission line is perpendicular to the antenna [Figure IV-2(a)], impedance variations over the radiating frequency band are minor, since this configuration minimizes the interactions between the fields from the antenna and transmission line. This impedance variation with frequency is very similar to the case in which the antenna is driven directly by the balun, as shown in Figure III-7(a). The differences that do exist may be attributed in part to the fact that the transmission line is not perfectly lossless and in part to the inevitable mismatches that occur at the connection between the balun and transmission line and between the transmission line and antenna. When the transmission line is brought to within about 2 inches of the antenna, driving-point-impedance fluctuations appear over the radiating frequency band as shown in Figure IV-2(b). As the transmission line is brought closer to the antenna

* The radiating frequency band of the 12-inch antenna begins at 300 MHz and extends beyond 1500 MHz as discussed in Section III-D-3.

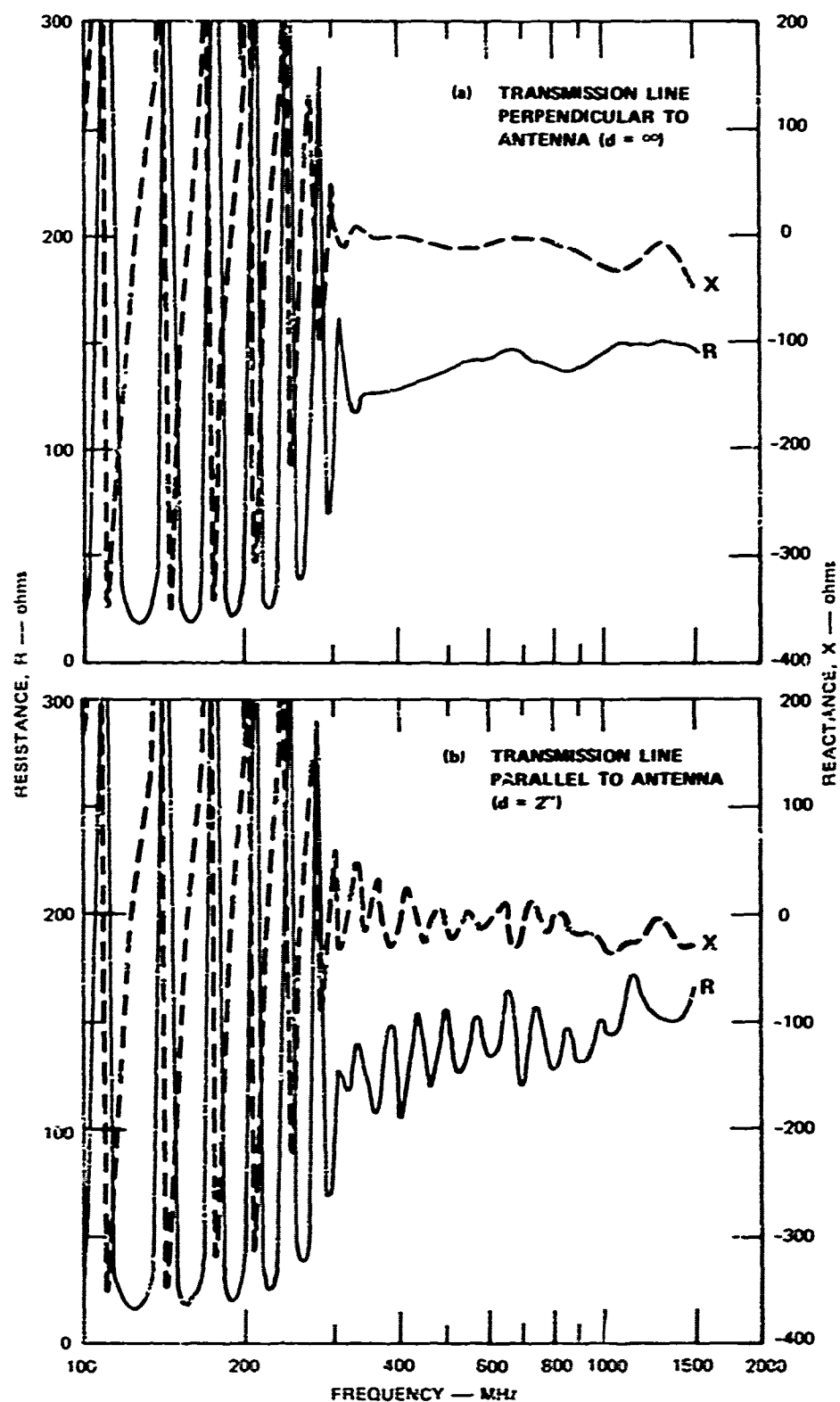


FIGURE IV-2 DRIVING-POINT IMPEDANCE OF THE 12-inch SPIRAL ANTENNA IN FREE SPACE FED BY MEANS OF A BALANCED TWO-WIRE TRANSMISSION LINE. The transmission line is connected to the metal side of the antenna at one end and driven by the 200-ohm Anzac balun at the other.

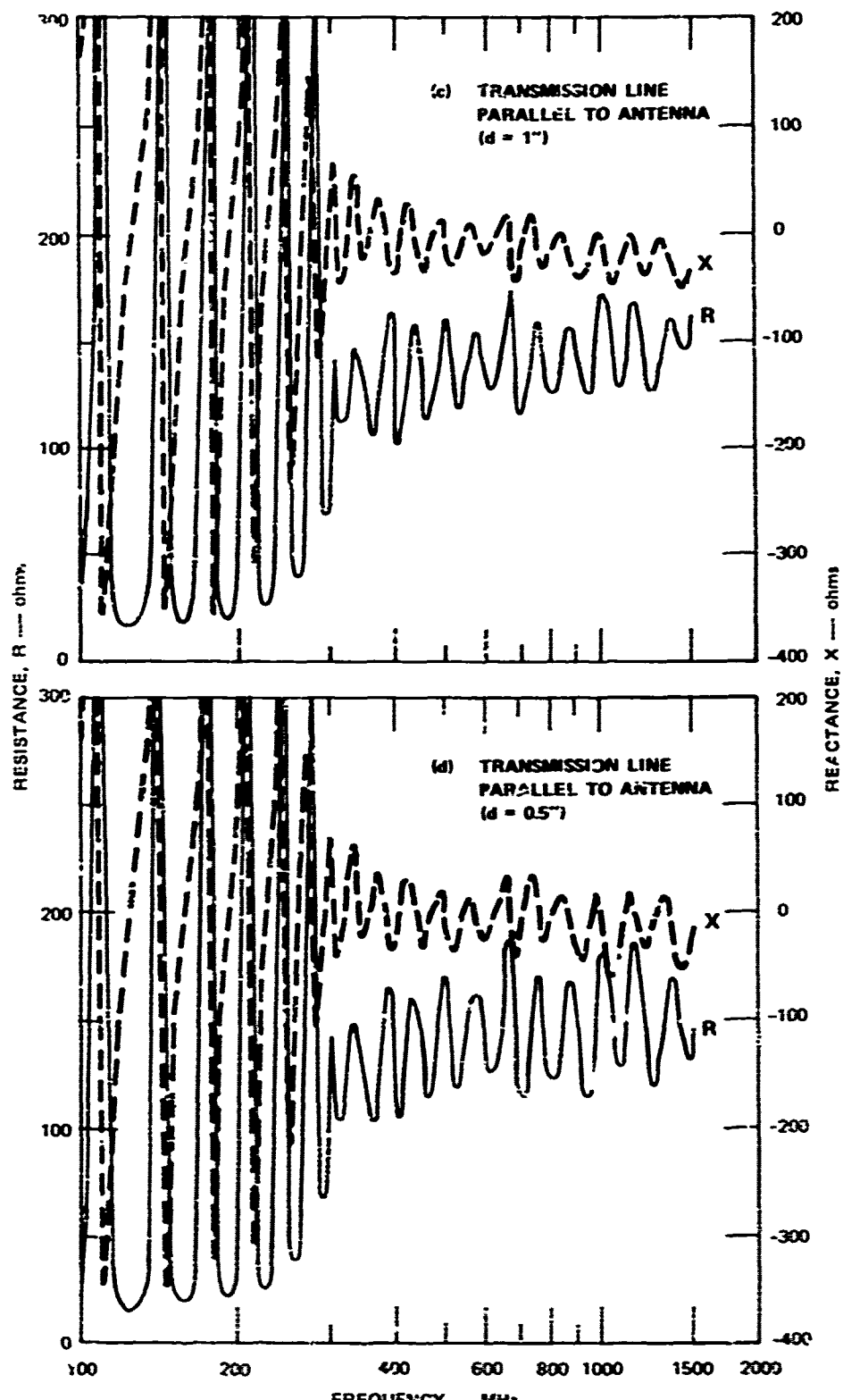
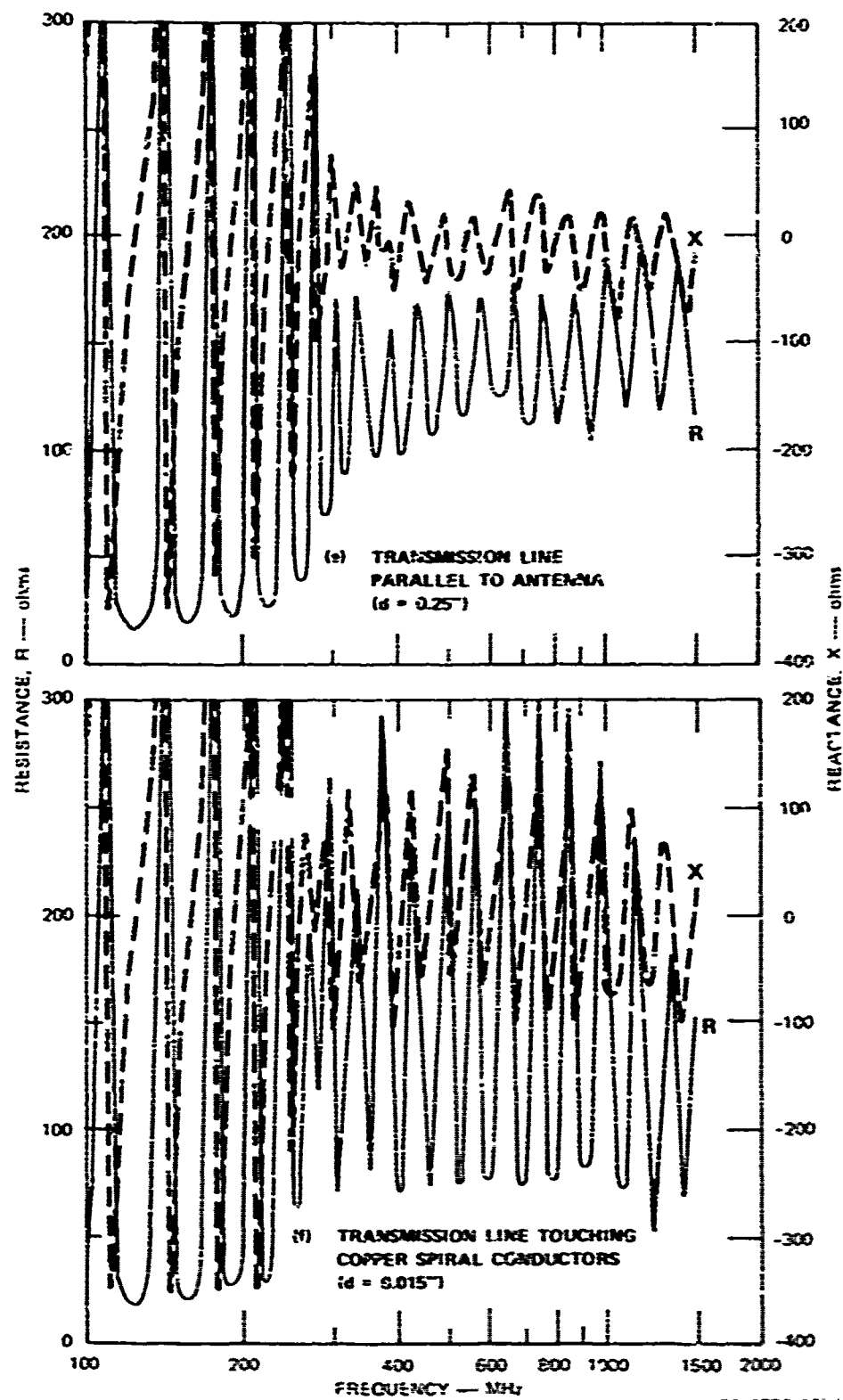


FIGURE IV-2 (Continued)



SA-1370-164c

FIGURE IV-2 (Concluded)

[Figures IV-2(c) through (e)] the fluctuations become greater and are greatest when the transmission line touches the antenna [Figure IV-2(f)].

The maximum VSWR within the radiating-frequency range of the antenna as seen at the antenna-feed terminals increases as the transmission line moves closer to the antenna. This parameter, relative to the average 12-inch-antenna driving-point impedance of 137 ohms (see Section III-D-3), is shown in Table IV-1 for the same transmission-line positions, d , represented in Figure IV-2. It is seen from the table that the maximum VSWR for the case when the transmission line touches the antenna is twice the maximum VSWR resulting when the transmission line is perpendicular to the antenna. The values of maximum VSWR in Table IV-1, however, are determined not only by the transmission-line and antenna field interactions, but by the mismatches that occur at the transmission-line connections to the balun and to the antenna. This is seen when comparing the maximum VSWR for the case when the transmission line is perpendicular to the antenna with the case when the antenna, situated in free space, is driven directly by the balun. In the latter case the maximum VSWR is 1.10, as was indicated in Section III-D-3. Comparing this value with the values in Table IV-1 gives one a somewhat quantitative measure of the adverse effect of running a transmission line, as shown in Figure IV-1, close to the antenna. However, this effect is seen more clearly when qualitatively comparing Figure III-7 with Figure IV-2.

One additional measurement was made to determine whether the transmission-line fields interacting with the antenna or the antenna fields interacting with the transmission line caused the most antenna driving-point-impedance degradation. The driving-point impedance of the 12-inch antenna was measured with the transmission-line feed perpendicular to the antenna [as in Figure IV-2(a)], but with a dummy transmission

Table IV-1

MAXIMUM VALUES OF VSWR OCCURRING IN THE RADIATING
FREQUENCY BAND OF THE 12-INCH ANTENNA FOR SEVERAL
ANTENNA/TRANSMISSION-LINE CONFIGURATIONS^a

Transmission- Line Position d (inches) ⁺	Corresponding Illustration	Maximum VSWR
=	Figure IV-2(a)	1.4
2.0	Figure IV-2(b)	1.4
1.0	Figure IV-2(c)	1.5
0.5	Figure IV-2(d)	1.6
0.25	Figure IV-2(e)	1.8
0.015	Figure IV-2(f)	2.8

^a The VSWR values are relative to 157 ohms and correspond to the maximum driving-point impedance values shown in Figure IV-2.

⁺ Defined in Figure IV-1

line, 6 inches long, fastened to the copper printed-circuit side of the antenna. The dummy transmission line ran from the center to the end of the antenna and was oriented so that the plane containing the two wire conductors was parallel to the antenna. The result was that driving-point-impedance fluctuations within the radiating frequency band of the antenna occurred with the same order of magnitude as the fluctuations that occurred for the case when the transmission-line feed was touching the antenna [Figure IV-2(f)]. Hence, it appears that the fields from the antenna reflected by the transmission line back to the antenna cause the most significant degradation of the antenna driving-point impedance.

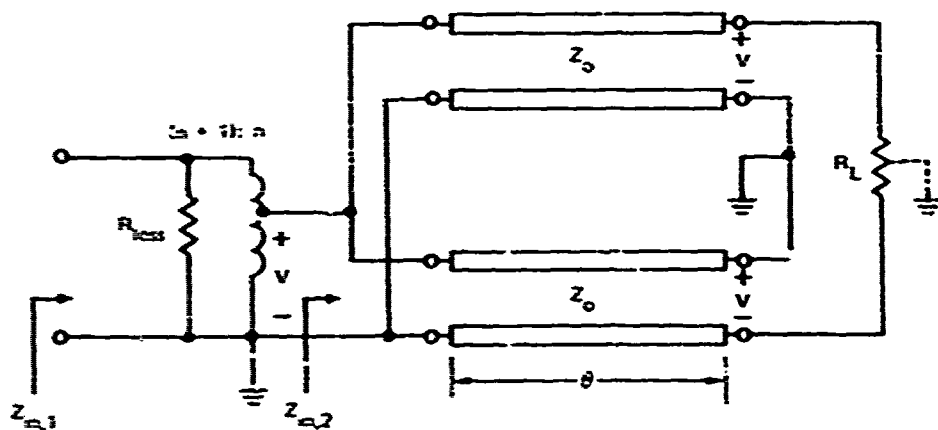
It is seen, then, that significant driving-point-impedance fluctuations within the radiating frequency band occur when the antenna is fed using a two-wire transmission line and when this transmission line is close to the antenna. Such fluctuations, of course, give rise to higher VSWRs at the antenna-feed terminals relative to the average driving-point impedance of the antenna. To maintain a low profile when the antenna is connected to its matching network (compact balun), it is necessary to run the transmission line that connects the antenna to the matching network, close to the antenna. Thus, a trade-off exists between the low-profile and low-VSWR requirements. In essence, the distance the transmission line is kept from the antenna is determined by the acceptable VSWR level at the center terminals of the antenna.

V DESIGN OF THE COMPACT BALUN

A. Theory

There were two principal objectives to be met by the balun designed at SRI. The first was to provide a thin package consistent with the size of the SMA (OSM) coaxial connector. The second objective was to provide an impedance transformation from 132 ohms balanced to 50 ohms unbalanced, rather than 200 to 50 ohms. (The 132-ohm figure is the average of the measured driving-point impedances for the 12- and 24-inch spiral antennas over their respective radiating frequency bands, as was shown in Section III-D.) How these objectives were met will be explained in this section.

Consider first the electrical design of the balun. The equivalent circuit of the balun is shown in Figure V-1. There are essentially two parts to this balun, a 4:1 balun and an autotransformer. The pair of



SA-1370-19

FIGURE V-1 EQUIVALENT CIRCUIT FOR THE COMPACT BALUN

Preceding page blank

equal-length, equal-impedance transmission lines on the right in Figure V-1 form a balun with a 4:1 impedance transformation. The resulting input impedance, $Z_{in,2} = 132/4 = 33$ ohms, is then transformed up to near 50 ohms by the autotransformer on the left in Figure V-1. The operation of the 4:1 balun portion will be discussed first. The balanced load R_L should be excited so that at any instant in time one terminal is as far above ground potential as the other one is below ground potential. Thus, a ground-potential point exists at the middle of the load, and the effective resistance from each load terminal to ground is $R_L/2$. When the balanced load is properly excited, therefore, each of the two transmission lines is terminated by a resistance $R_L/2$. Choosing the characteristic impedance of each transmission line to be $Z_0 = R_L/2$, a condition of impedance match exists. Looking into the left-hand end of each transmission line, a pure resistance $R_L/2$ is also seen at all frequencies. Connecting the left-hand ends of the transmission lines in parallel gives a net input resistance of $R_L/4$.

The discussion to this point has implicitly assumed that each transmission line supports only the desired TEM mode, with equal but opposite currents flowing in its two conductors. That is, it has been assumed that each transmission line existed in free space with no other conductors near it. As the balun is constructed, of course, a ground plane exists near the transmission lines. Each transmission line can thus support a second TEM mode in which the currents in the two wire conductors are equal and in the same direction, with the return current flowing on the ground plane. In this mode, the two-wire transmission line is equivalent to a single, larger-diameter wire over ground. This undesired mode can be suppressed by threading several toroidal beads of ferrite along the length of the transmission line, with both wire conductors passing through the hole of each toroid. With the undesired-mode current passing through the bead centers, and the return current

flowing outside the beads, the undesired mode couples strongly to the ferrite material. At sufficiently low frequencies such that the ferrite has high permeability, the characteristic impedance for the undesired mode is raised. When this impedance is made much higher than other circuit impedances, very little power is coupled into the undesired mode. At higher frequencies where the permeability of the ferrite decreases, the ferrite becomes very lossy and introduces high resistance in series with the undesired-mode current. This not only dissipates any energy existing in the undesired mode, but also reduces the amount of energy converted to the undesired mode.

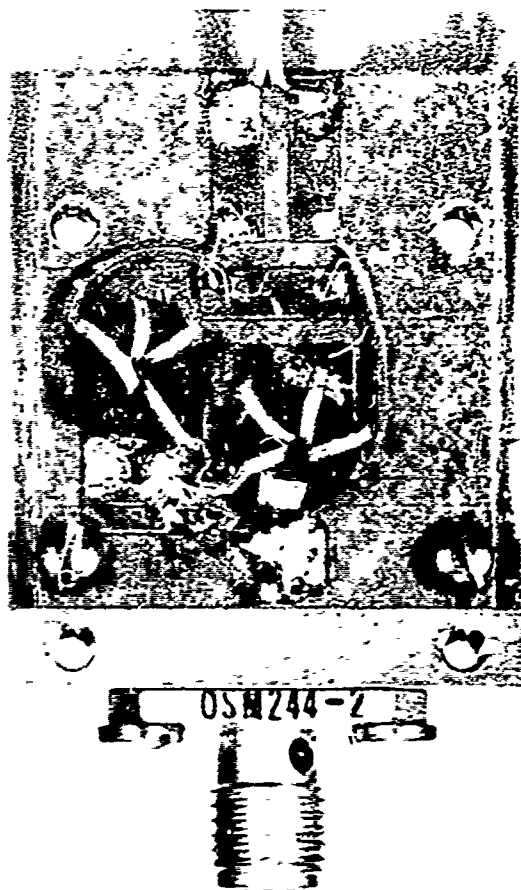
Returning to discussion of the balun equivalent circuit, note that the upper transmission line in Figure V-1 has the same wire grounded at both ends of the line. If geometrical symmetry of the line is maintained, there will not be any tendency for energy to couple from the desired two-wire-line mode to the undesired mode. On the other hand, the lower transmission line in Figure V-1 has one wire grounded at the left, and the other wire grounded at the right. This will produce strong coupling of energy from the desired mode to the undesired mode. For proper operation of the balun it is essential that the lower transmission line be surrounded by ferrite in order to suppress the undesired mode.

Note that even with the transmission line threaded through the ferrite beads, the desired two-wire-line mode is not affected much by the ferrite. This is because the magnetization of the ferrite that would be caused by the current in one wire is canceled by the opposite current in the other wire. In order that the slight effect of the ferrite on the desired mode be equal for each transmission line, ferrite is used around both transmission lines. This preserves equal characteristic impedance, electrical length, and loss for the two transmission lines.

The above discussion suggested using several ferrite toroids along the length of the two-wire line to suppress an undesired mode. The same performance can be obtained by winding each two-wire line several turns through a single ferrite toroid, as shown in Figure V-2. The equivalence between the two geometries holds as long as the RF signal current is small enough that the ferrite is not saturated. The single-toroid, multiple-turn approach was used here for compactness. The result resembles a bifilar-wound transformer more than a transmission line, and indeed the electrical performance can also be explained using transformer theory.

The other portion of the compact balun, the autotransformer, will now be discussed. To step up the 32-ohm impedance of the 4:1 balun to 50 ohms, the transformer should have a turns ratio of $\sqrt{50/32} = 1.25 = 5/4$. This is a particularly fortunate requirement for turns ratio. It has been found by experience that autotransformers with turns ratios of the form $(n + 1)/n$ can be constructed to be very broadband. In fact they can be built having no inherent frequency-limiting elements such as inductors, capacitances, or transmission-line stubs. This is not the case for arbitrary choice of turns ratio. The practical frequency limitations are set by the properties of the ferrite core on which the autotransformer is wound. The high-frequency limit is set by increases in core dissipation loss. The low-frequency limit is set by the inductive reactance of the windings. The windings appear as a short circuit at zero frequency. The higher the core permeability, the lower in frequency will be the lower edge of the operating band. A large number of turns also helps, within limits, but is inconsistent with other requirements.

The autotransformer could be wound on its own ferrite toroidal core. It was, however, wound on the same toroid as was the lower



(a) TOP VIEW WITH LID REMOVED
EXPOSING ELECTRIC CIRCUIT



(b) SIDE VIEW

SA-1370 20

FIGURE V-2 COMPACT BALUN

transmission line in Figure V-1. This resulted in lower overall dissipation loss than if separate cores had been used, and also resulted in a more compact device. That a core can be shared for two portions of the balun can be explained qualitatively as follows. Note that from the tap on the autotransformer to ground there is a voltage drop V . This same voltage drop also exists between the left- and right-hand ends of the lower transmission line in Figure V-1. If, then, the transmission line is wound through the core n times, the lower n turns of the autotransformer can be wound on the core in the same direction.

In constructing the autotransformer, the impedance between successive turns should, in theory, be varied in a controlled manner. In practice it is adequate to make the top turn relatively low impedance and the remaining turns high impedance. This is accomplished by using a wide strip as the first (top) turn, and fine wire for the remaining turns. The fine wires are wound on the core first, and the wide strip is wound on top of the wires. The tap of the autotransformer is a metal island on the printed circuit board that also supplies the other connection points of the balun. Only the strip making up the top turn is visible in the photograph of Figure V-2.

One other important element in Figure V-1 is the resistance representing the dissipation loss of the autotransformer core. To a good approximation, the value of this resistance can be calculated as a constant times the square of the number of turns. For the ferrite cores used, this constant is 10 ohms per turn squared, giving $R_{loss} = 250$ ohms for five turns. If separate ferrite cores were used for the autotransformer and for the transmission line, a second loss resistance would also be introduced into the equivalent circuit.

B. Choice of Parameters

The preceding section presented the theory behind the balun design. This section will discuss the choice of the parameters of the baluns constructed.

As mentioned above, the two transmission lines in the balun should be identical. That is, they should have equal characteristic impedances, losses, and electrical lengths. The characteristic impedance should be $132/2 = 66$ ohms, since the average load impedance is 132 ohms, as determined in Section III-D. It would be possible to construct a 66-ohm line by twisting a pair of wires of correct diameter and of correct insulation thickness. Obtaining the correct geometry could be done empirically. In order to ensure good reproducibility, however, a commercially available two-wire line was used even though its impedance was not exactly 66 ohms. The line used is Type C05A080 manufactured by W.L. Gore and Associates, Flagstaff, Arizona. This two-wire line has a rated impedance of 75 ohms, but the actual impedance is slightly higher, especially when wound on the ferrite core. Data presented below infer an impedance of 85 ohms.

The ferrite toroids used in the compact balun are Type F303-1 Q-1 manufactured by Indiana General Corporation, Keasbey, New Jersey. These have an outside diameter of 0.230 inch, an inside diameter of 0.120 inch, and a thickness of 0.060 inch. Toroids of the same size made of Q-2 material were also tried. The Q-2 material has slightly lower loss than Q-1 material, but also has lower permeability. The latter property caused the input VSWR at the lower bandedge of the balun to degrade slightly to 1.5. A VSWR of 1.2 was achieved at 100 MHz using the Q-1 material.

In Section V-A, a turns ratio of 5:4 was calculated based on transforming 32 ohms to 50 ohms. Taking the loss resistance into account,

however, the 5:4 turns ratio does not necessarily give the best input VSWR. Looking into the balun, the 50-ohm generator sees the parallel combination of the transformed load impedance and the loss resistance. The results of using various turns ratios, limited to the desired $(n + 1):n$ relationship, are summarized in Table V-1. It is seen that with a loss constant of 10 ohms per turn squared, the choice of turns ratio does not greatly influence the parallel combination. Turns ratios of 7:6, 6:5, and 5:4 were tried, with the latter ratio giving the best measured performance over the 100-to-1500-MHz band. Less dissipation loss could be obtained by using larger toroids, but at the expense of increasing the balun size.

Table V-1
COMPARISON OF TURNS RATIOS

Turns Ratio	Transformed 32-Ohm Impedance (ohms)	Loss Resistance (ohms)	Parallel Combination (ohms)
3:2	72	90	40
4:3	57	160	42
5:4	50	250	42
6:5	46	360	41
7:6	44	490	40

In order to achieve the desired flat form factor for the compact balun, the balun was constructed on a planar printed circuit board, as shown in Figure V-2. On the circuit board are metal islands for soldering the various balun connections, and that also provide some

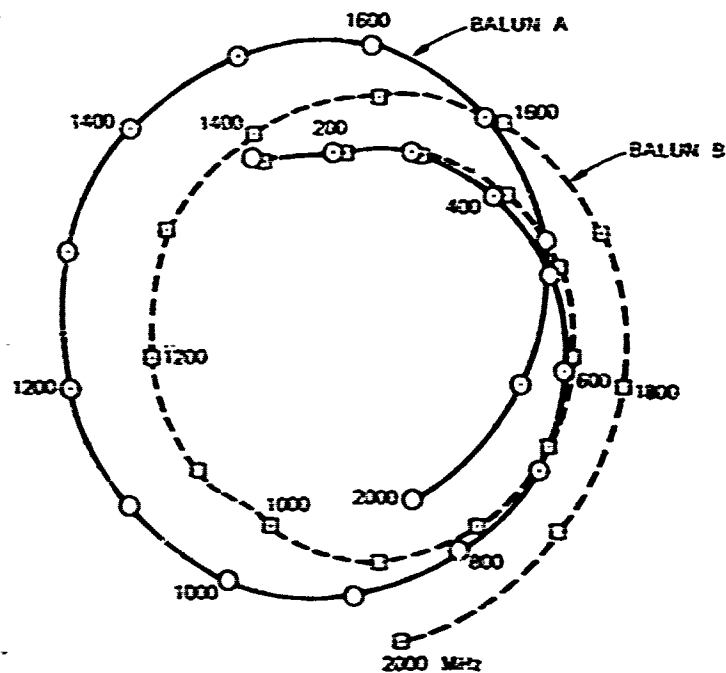
empirically determined capacitances. The circuit board is 1/16-inch Duroid 5880 manufactured by Rogers Corporation, Rogers, Conn. The circuit board is mounted over a brass ground plane, which is integral with the mounting surface for the SMA (model OSX 244-2) coaxial connector. The total balun thickness is such that the coupling nut that screws onto the connector just has clearance to turn. The balun could be made as thin as 1/8 inch if no coaxial connector was used, but a miniature coaxial cable was permanently attached to the balun.

C. Measured Characteristics

In this subsection measured data will be presented for the two compact baluns terminated by the 132-ohm resistive load shown in Figure II-2. A comparison will also be made with calculated input impedance based on the equivalent circuit of Figure V-1. The characteristics of the combination of the baluns and the spiral antennas are presented in Section VI.

The measured input impedances are shown as functions of frequency in the Smith chart plots of Figure V-3, and the real- and imaginary-part plots of Figure V-4. Even though the input impedance of the balun varies with frequency, the VSWR is fairly constant and reasonably low at about 1.3. The resistance minimum is determined by the core loss, as discussed in connection with Table V-1 above. The impedance loci swing around the Smith chart mainly because the transmission lines in the 4:1 balun portion do not have the correct impedance of 66 ohms.

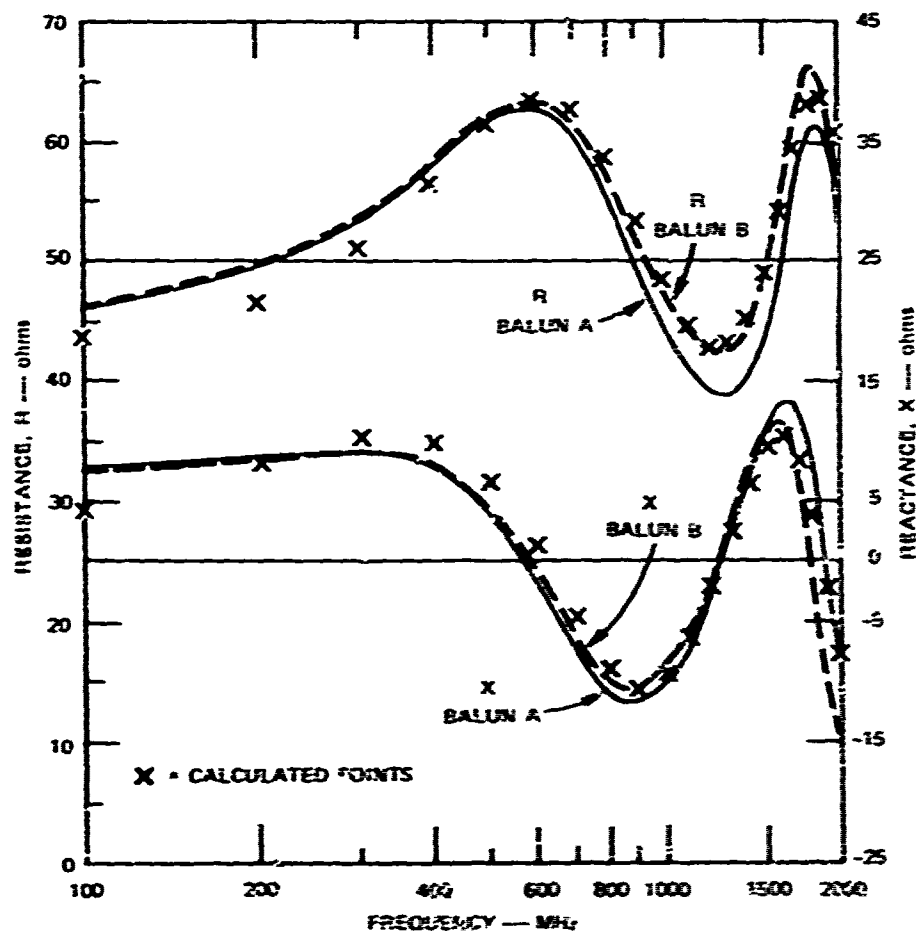
That the observed input-impedance characteristics can be explained fairly well on the basis of the core loss and the incorrect line impedance, is confirmed by the calculated points shown in Figure V-1. These points were obtained for the equivalent circuit of Figure V-1, using core-loss resistance $R_{\text{loss}} = 250$ ohms, an autotransformer turns



$\frac{Z}{50}$

SL-1373-71

FIGURE V-3 SMITH-CHART IMPEDANCE PLOT FOR COMPACT BALUNS TERMINATED IN A MATCHED 132-ohm LOAD



SA-1370-22

FIGURE V-3 REAL AND IMAGINARY PARTS OF INPUT IMPEDANCE OF THE COMPACT BALUNS TERMINATED IN A MATCHED 132-ohm LOAD

ratio of 5:4, line impedances $Z_0 = 85$ ohms, and line lengths of half wavelength at 1240 KHz. The calculations did not take the following into account: the variations, with frequency, of the ferrite toroid permeability and loss; the fact that the autotransformer departed from ideal; the fact that the ferrite toroids did not completely suppress the undesired mode between each transmission line and ground; and the small coupling between the two transmission lines. Even so, the calculated points agree very well with the measured curves.

If 66-ohm transmission line were available for constructing the balun, the impedance loci in Figure 7-3 would be clustered around the point $0.8 \pm j0$. The peak VSWR would not, however, be much better than that shown at the bottom of Figure V-5. The insertion loss shown at the top of Figure V-5 is primarily due to dissipation loss in the miniature ferrite toroids. Loss could be reduced by using larger toroids, but the balun would then be larger.

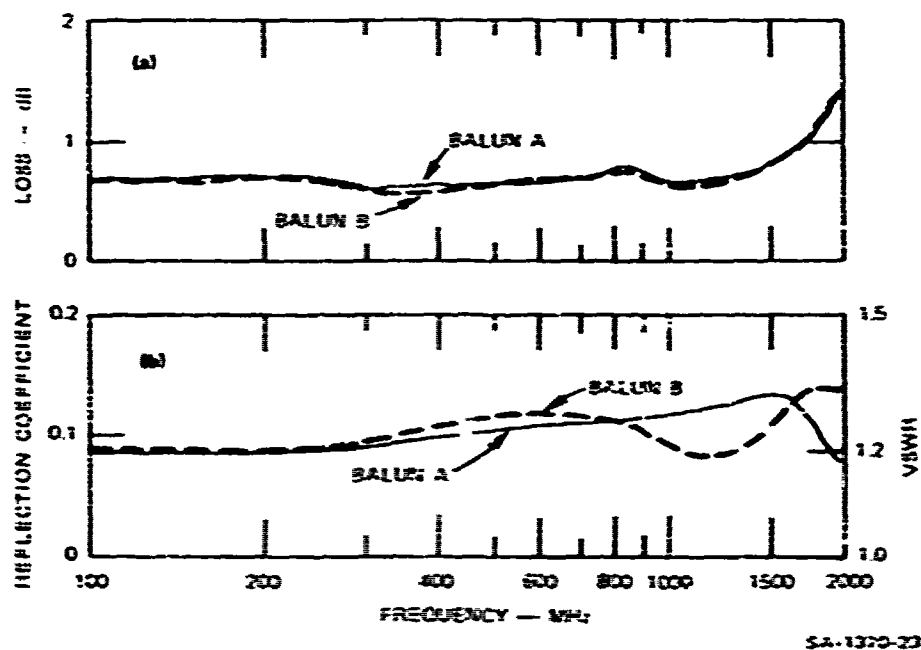


FIGURE V-5 REFLECTION DATA AND TRANSMISSION LOSS FOR THE COMPACT BALUNS TERMINATED IN A MATCHED 132-ohm LOAD

VI INPUT-IMPEDANCE AND REFLECTION DATA FOR COMPACT BALUN/ANTENNA CONFIGURATIONS IN FREE SPACE

A. General

The impedance looking into the unbalanced port of the compact baluns (Section V) was measured for two balun/antenna configurations, one with the 12-inch and one with the 24-inch antenna. Free space was chosen as the representative environment under which the measurements were obtained. This was because the various building materials, described in Section III-C, had little effect on the driving-point impedance of either antenna when placed against them, for the reason discussed in Section III-D. The two compact baluns were designed, as specified by the sponsor, to match the average driving-point impedance of each antenna to a 50-ohm-system impedance. Although practically identical (both physically and electrically), these baluns were arbitrarily labeled A and B (as indicated on Figures V-3 and V-4) and were consistently used with the same antenna throughout the measurements of the balun/antenna configurations. Balun A was used in conjunction with the 12-inch antenna and Balun B was used in conjunction with the 24-inch antenna.

In both of the balun/antenna configurations the balun was connected to its spiral antenna by means of a twin-lead transmission line^{*} of length equal to approximately the radius of the antenna. The measured characteristic impedance of the transmission line was 132 ohms, which is the balanced-port-impedance of the baluns.

* Gore C05A060; manufacturer-specified characteristic impedance is 125 ohms.

Several balun/antenna configurations are possible, but their choice depends primarily on two factors--system sensitivity, and the balun/antenna-configuration profile. These configurations, including the two configurations chosen for measurement, are discussed in the following subsection. To improve the balun/antenna configuration impedance match to the 50-ohm system impedance at frequencies below the radiating frequency band (see Section III-A), the outer ends of the antennas were terminated with a combination lumped and distributed load. These terminations are discussed in Subsection VI-C. Finally, the results of the impedance measurements for the two balun/antenna configurations situated in free space are discussed in Subsection VI-D.

B. Balun/Antenna Configurations

The balun may be connected directly to the center of the antenna, or it may be connected remotely by use of a balanced transmission line. When connected directly to the antenna, the balun may be mounted lengthwise either perpendicular or parallel to the antenna. When the balun is mounted perpendicular, its balanced-port microstrip transmission line (see Figure 1-2) can be extended by means of pins that would plug directly into the antenna. The length of the balun (2 inches), however, would preclude a low-profile configuration in this case. When the balun is mounted parallel to the antenna, a low profile is achieved,^{*} but an increase in VSWR at the center terminals of the antenna would result due to radiating-field reflections from the relatively large metal surface of the balun close to the antenna. The net effect of this increase in VSWR is loss of system sensitivity, because more of the

* Equal to 0.435 inch (antenna circuit-board thickness, 0.05 inch, plus balun thickness, 0.375 inch).

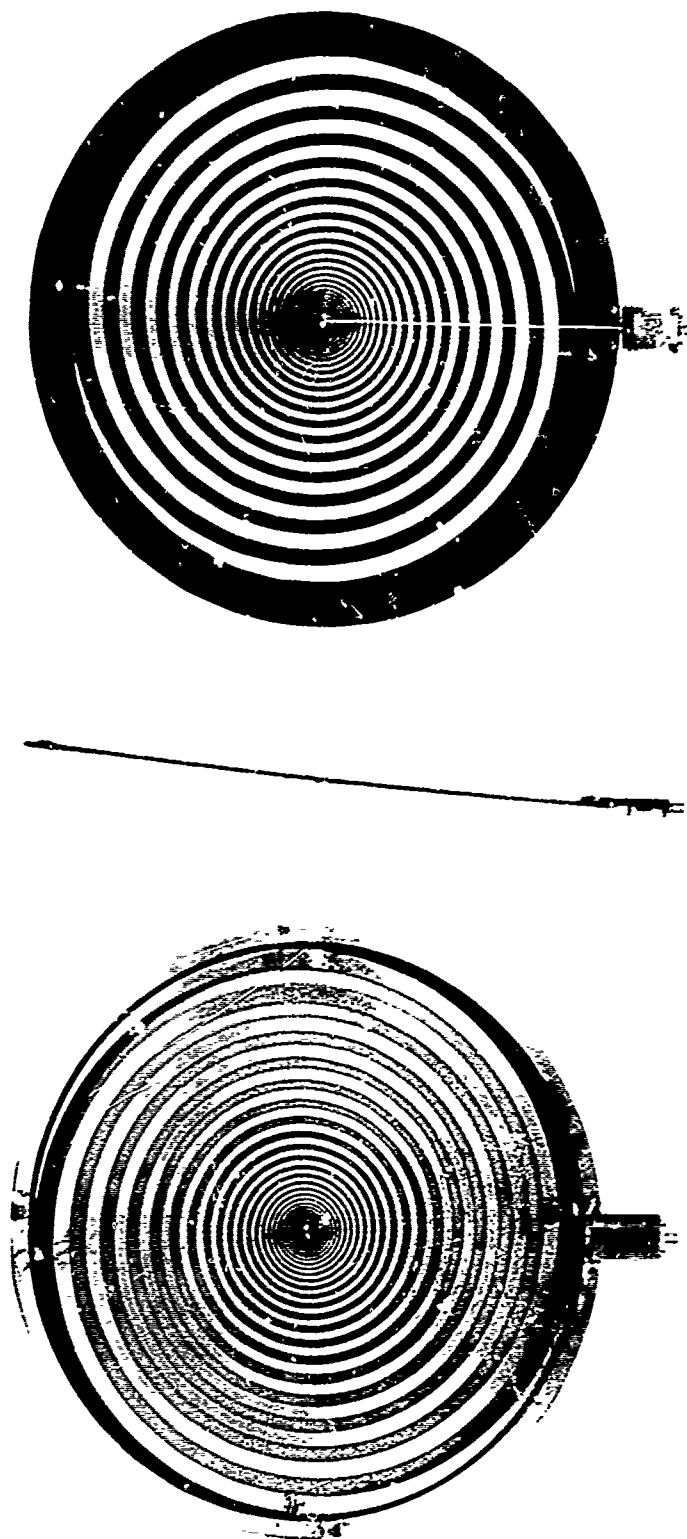
signal received by the antenna is reflected back into free space. In addition, the pins needed to extend the balun balanced-port microstrip transmission line for connection directly to the antenna would have to be mounted at right angles to the microstrip conductors. This would result in significant reflections at the pin-microstrip connections, thus contributing an additional loss in system sensitivity. Furthermore, sufficient physical support for the balun would be difficult to achieve in either case when the balun is connected directly to the antenna center.

The alternative of remotely connecting the balun to the antenna through use of a transmission line alleviates the problem of loss of system sensitivity due to the close proximity of the balun to the antenna. However, as discussed in Section IV, the transmission line causes its own problems, depending on its position relative to the antenna. The least amount of interaction between the radiating fields and transmission line occurs when the transmission line extends perpendicularly from the center of the antenna. This is the case that applied to Figure IV-2(a). Here, the balun is positioned far enough away from the antenna so that its effects on the driving-point impedance of the antenna are negligible. However, it is obvious that for this arrangement, the low-profile requirement for the balun/antenna configuration is not met.

From a low-profile as well as practical standpoint the ideal place to position the balun is at the edge of the antenna. Here, the balun is situated in the plane of the antenna where radiation fields do not exist. Furthermore, the balun may be conveniently attached to the outer metal ring of the antenna for solid support. This arrangement requires, of course, that the transmission line, connecting the antenna to the balun, be very close to the antenna, which causes significant

interaction between the radiating fields and the transmission line, with a resulting loss in system sensitivity. As will be seen subsequently, however, this loss in system sensitivity amounts to only about 0.5 dB more than for the case when the transmission line extends perpendicularly from the antenna.

The two configurations used for the impedance and reflection measurements discussed in this section were the ones incorporating the remote balun arrangement. The twin-lead transmission line was connected directly to the balun balanced-port-microstrip conductors at one end and to the non-conductor side of the antenna at the other end. In the first configuration the transmission line extended perpendicularly from the center of the antenna. Its length, as previously indicated, approximately equaled the radius of the antenna used in the configuration. The purpose of the measurements for this configuration is to show how well the balun matches the specified 50-ohm system impedance to the antenna-driving-point impedance over the radiating frequency band. Because the antennas were appropriately terminated, improvement in the antenna match at frequencies below the radiating frequency band was expected. A second purpose of these measurements is to observe this improvement. For the first configuration both the balun and transmission line influence the driving-point impedance of the antenna very little. In the second configuration the balun was attached to the outer metal ring of the antenna. The transmission line ran parallel to the antenna and was separated from the metal spiral conductors by the dielectric circuit board. This corresponds to a distance, d , of 0.078 inch in Figure IV-1. The arrangement of the second configuration is shown in Figure VI-1. The purpose of the measurements for this configuration was to show the overall effect on the impedance of the balun/antenna configuration as well as the effect on system sensitivity when the transmission line is close to the antenna. It is this configuration that achieves the lowest profile.



SA-1370-24

- (a) TOP VIEW SHOWING SPIRAL CONDUCTORS AND RESISTOR TERMINATION
- (b) SIDE VIEW SHOWING LOW PROFILE
- (c) BACK VIEW SHOWING TWIN LEAD TRANSMISSION LINE CONNECTING BALUN AND ANTENNA, AND DISTRIBUTED LOAD TERMINATIONS

FIGURE VI-1 COMPACT BALUN ATTACHED TO OUTER METAL RING OF 12-INCH ANTENNA. Twin-lead transmission (Gore CO5A060) connects balun to antenna center input terminals. Antenna is terminated with combination lumped and distributed load.

C. Termination for the Antenna Outer Ends

Terminating networks were placed at the outer ends of the antenna spiral conductors in order to improve the input VSWR for frequencies below the radiation band. At these frequencies, current reaches the spiral ends, is reflected from the ends, and emerges again from the drive terminals at the antenna center. This produces high input VSWR if the outer ends are not terminated properly.* Data were measured on a previous contract¹ to determine what type of terminating network should be used between the spiral outer ends and the metal ring that exists around the periphery of the circuit board on which each antenna is printed. It was concluded that lumped-element terminations could be used to reduce the reflection at frequencies well below the radiation cutoff frequency. However, at and just below radiation cutoff, distributed loss is required in order to damp out a resonance that is related to the path length around the metal-ring circumference, and is discussed in Section III-B of Ref. 1. Each termination finally used on the spiral outer ends consists of a combination of a lumped resistor and distributed-resistance cloth material.

In tracing the development of the final terminations, the use of lumped R-L-C networks without distributed loss will first be discussed. The impedance measured at the outer spiral ends is shown in Figures 5 and 6 of Ref. 1 for the 12- and 24-inch antennas, respectively. Averaging out the ripples in the curves in those figures,⁺ it is found that the

* Within the radiation frequency band, on the other hand, most of the power is radiated and very little current reaches the spiral ends. The terminations on the spiral end then have negligible effect on the input VSWR.

⁺ These ripples are not a property of the antenna, but are a result of the conditions under which the measurements were made. See Ref. 1, p. 50, for a discussion of this subject.

outer-end impedance can be represented at low frequencies as a 180-ohm resistor in series with an inductor. This representation is valid up to about 200 MHz for the 12-inch antenna, and up to about 100 MHz for the 24-inch antenna. At higher frequencies, a transmission-line stub must be used in the equivalent circuit instead of a lumped inductor.* Considering, for now, only the lower frequencies, the equivalent series inductances are 160 and 320 nH for the 12- and 24-inch antennas, respectively. The design of impedance-matching networks for series R-L loads is discussed by Matthaei, Young, and Jones.⁹ Using their procedure, networks of varying degrees of complexities were designed to terminate the 12-inch-antenna ends with minimum reflection up to 200 MHz. These networks and their calculated performances are shown in Figure VI-2.⁺ This figure shows that the $n = 3$ and $n = 4$ networks reduce the reflection by a factor of between 2 and 4.5 as compared to a simple resistor ($n = 1$) for frequencies below 200 MHz.[†] As is typical of impedance-matching networks, going from $n = 3$ to $n = 4$ gives only slight improvement in performance.

* As is discussed in Section III-B of Ref. 1, the equivalent transmission-line stub, or the series inductance, is due to the length around the circumference of the metal ring at the edge of the antenna. Each matching network is to have one terminal connected to an end of the spiral, and the other terminal connected to the metal ring. The resistive component is the antenna radiation resistance.

⁺ A separate network is required at each of the two spiral ends of the antenna. Since the spiral is driven in a mode balanced with respect to ground (equal but opposite currents), half of the 180-ohm and 160-nH values mentioned before can be associated with each spiral end. Thus the 90-ohm and 80-nH values appearing on Figure VI-2.

[†] The value of n refers to the number of reactive elements, including that in the load to be matched. This follows the notation of Ref. 9.

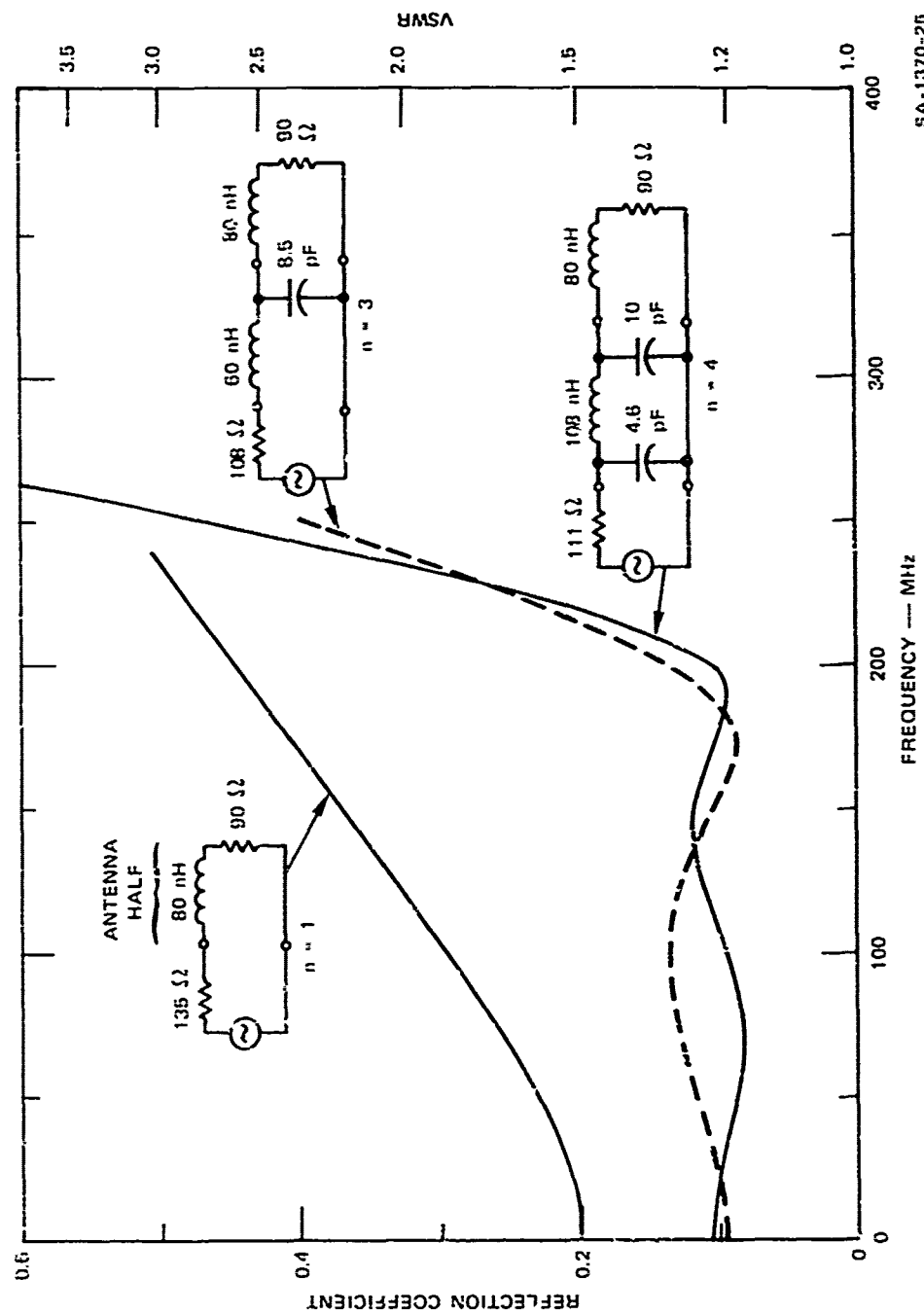


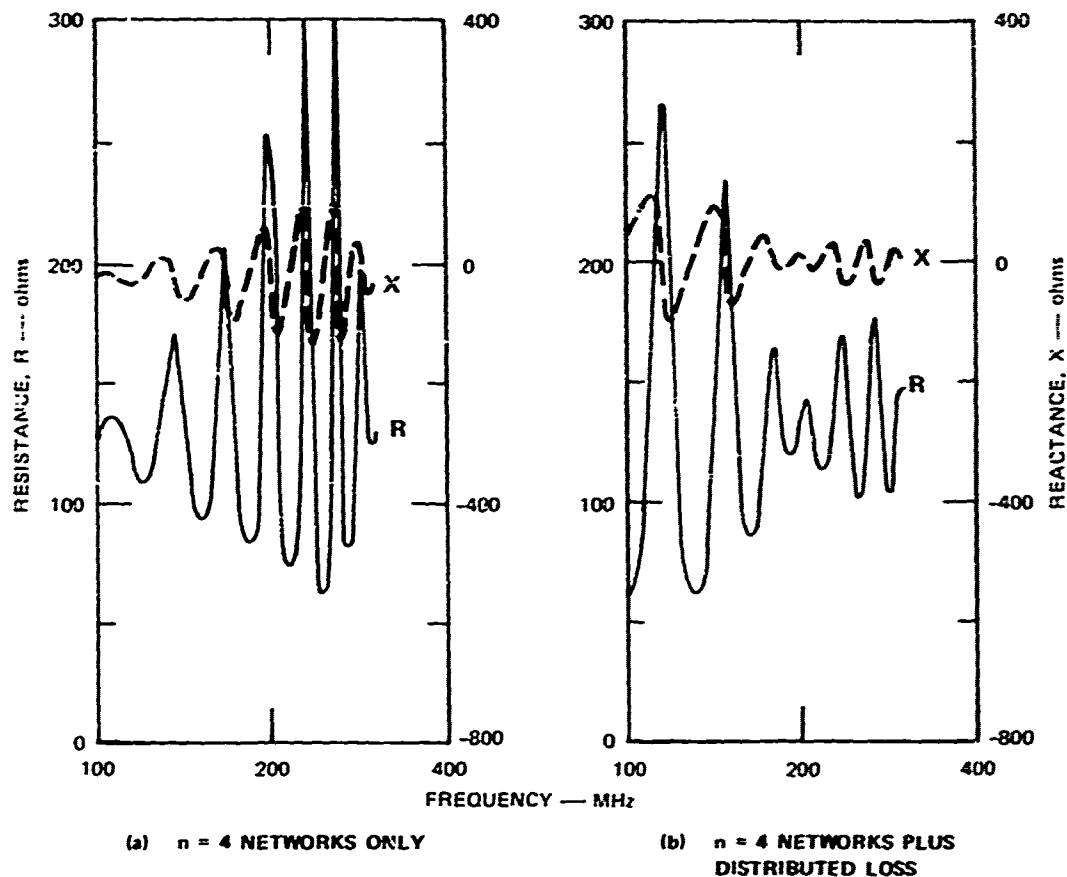
FIGURE VI-2 CALCULATED PERFORMANCE OF MATCHING NETWORKS FOR 12-INCH-ANTENNA OUTER ENDS

The schematics on Figure VI-2 are drawn as if a generator at each spiral outer end were driving the antenna. (Indeed, this was the way the networks were designed.) In actual use, however, the generator resistance shown is to absorb power from the spiral conductor when the antenna is excited from its center. The networks will still perform properly when driven this way. It is a fundamental property of reciprocal, lossless^{*} networks that the reflection-coefficient magnitude is the same when the network is driven from either end. If the voltage of the generator shown in Figure VI-2 were set to zero, and another generator inserted in series with the 90-ohm resistor, the reflection coefficient then calculated looking toward the left from the junction of the 90-ohm resistor and the 80-nH inductor would be the same as plotted in Figure VI-2.

Figure VI-2 applies to the 12-inch-diameter spiral. The 24-inch spiral is essentially a 2:1 scaled-up version of the smaller antenna. Thus, Figure VI-2 can be applied to the 24-inch antenna by multiplying all inductances and capacitances by 2, and dividing the number along the frequency axis by 2. The reflection and VSWR scales and the curves remain unchanged.

A pair of the $n = 4$ networks were built for the 12-inch antenna. The resistors were 110-ohm, 1/4-watt carbon, the capacitors were 10- and 5-pF mica, and the inductors were 7.5 turns of AWG-30 enamel wire close-wound on the resistor. These networks were soldered from the outer end of each spiral to the metal ring around the periphery of the antenna. The impedance measured at the center drive points of the spiral is shown in Figure VI-3(a). Only the frequencies below the

* The only dissipation loss shown in Figure VI-2 is in the load and generator resistances.



SA-1370-23

FIGURE VI-3 DRIVING-POINT IMPEDANCE OF THE CENTER OF THE 12-INCH SPIRAL ANTENNA WHEN THE OUTER ENDS ARE TERMINATED WITH $n = 4$ NETWORKS

radiation cutoff of about 300 MHz are of interest here. Comparing Figures III-7(a) and VI-3(a), it is seen that the terminating networks do reduce the fluctuations in impedance significantly. The impedance is nearly constant near 100 MHz, and presumably improves even more at lower frequencies. The impedance fluctuates more just below 200 MHz than was expected based on Figure VI-2. This is presumably due to the approximation made in representing the measured antenna impedance as a simple R-L load. As expected, there is still appreciable impedance variation at frequencies just below radiation cutoff.

In order to damp out the impedance fluctuations near the radiation cutoff frequency, distributed loss was added to the spiral outer ends. This loss is in the form of a ring of carbon-impregnated fabric* that is 11.25 inches inside diameter so as to completely cover the last half turn of the gap between each spiral arm and the outer metal ring. The lossy cloth partially fills the preceding quarter turn of the gap in the form of a smooth taper. The lossy cloth is cemented to the opposite side of the circuit board from the copper conductors. The coupling to the antenna is thus by means of its electric field. Ohmic contact was avoided so that the lumped networks could act as the termination at low frequencies.

The antenna impedance measured after adding the distributed loss is plotted in Figure VI-3(b). The distributed loss was very effective in smoothing the impedance between 200 and 300 MHz. Near 100 MHz, however, the distributed loss degraded the match of the lumped network. The distributed loss was left on the antenna on the assumption that good impedance match just below the radiation band is more important than at lower frequencies.

After the data of Figure VI-3 were taken, the $n = 4$ lumped networks were replaced by simple 110-ohm resistors. The 100-MHz match was only slightly degraded, so it was not considered worthwhile to use the more complex networks. The distributed loss by itself is not as good a termination as the combination of distributed and lumped losses. It was found that the impedance match degraded slightly at all frequencies below 300 MHz if no network was connected from the spiral ends to the outer metal ring.

* The lossy cloth has a resistance of 200 ohms per square. It is Eccosorb SC-200 manufactured by Emerson and Cuming, Canton, Mass.

Further improvement in the low-frequency match could be obtained by measuring again the impedance existing at the spiral outer ends now that the distributed loss has been added to the antenna. A new network could then be designed. Use of cloth with different resistivity, and using slightly different geometry might also give improvements. The time schedule did not permit trying these refinements.

A parameter that was not measured is the antenna gain. At frequencies just above 300 MHz, the distributed loss probably reduces the gain slightly, because some of the power at these frequencies that would otherwise be radiated is absorbed. The inside diameter of the lossy cloth was made as large as possible, consistent with good damping of the impedance from 200 to 300 MHz. At frequencies well above the radiation cutoff, the presence of the lossy cloth would have no influence on the antenna gain or pattern.

D. Measured Data for the Balun/Antenna Configurations

The results of the impedance and reflection measurements obtained for the two balun/antenna configurations described in Section VI-B are presented here. The purpose of these measurements is to show the overall impedance characteristics, at frequencies from 100 to 2000 MHz, for both the 12-inch and the 24-inch spiral antennas. The improvement in the impedance match between a 50-ohm system and the antenna over the radiating frequency band is shown when the compact balun is used to transform the driving-point impedance of the antenna to the system impedance. An improvement is also observed in the impedance match at frequencies below the radiating frequency band due to appropriately terminating the antennas, as discussed in the preceding subsection. Finally, the effects on impedance and system sensitivity are shown when the balun is attached to the outer metal ring of the antenna where the

transmission line connecting the antenna to the balun is very close to the spiral conductors. As mentioned previously, this latter configuration is the one that gives the lowest profile characteristic.

The impedance and reflection data for both configurations are shown in Figures VI-4 through VI-7 for the 24-inch antenna, and Figures VI-8 through VI-11 for the 12-inch antenna. The data are shown plotted as a function of the log of frequency and are also shown plotted on Smith charts. The reflection coefficient (from which impedance is derived) was measured at the unbalanced port of each compact balun. The measured reflection data are relative to the specified impedance of 50 ohms. The Smith-chart plots are shown normalized to this same impedance and cover the radiating frequency band of their respective antennas. The Smith-chart plots for the configuration where the transmission line is close to the spiral conductors (Figures VI-7 and VI-11) are not continuous plots but rather point plots. This is because the rapid fluctuations of antenna impedance with frequency, due to the close proximity of the transmission line to the antenna, cause numerous loops on the Smith chart. The loops are so numerous that, over the radiating frequency band, they overlap and coincide at various frequencies, making a continuous plot very difficult, if not impossible, to follow. Thus, for this configuration, a number of impedance points at discrete frequencies are plotted to show the impedance spread over the radiating-frequency range of the antenna rather than a continuous curve over the same frequency range.

As mentioned previously, significant improvement occurs in the impedance match between a 50-ohm system and both the 24-inch and the 12-inch antenna when the compact baluns are used to transform the antenna driving-point impedances to the system impedance. This is evident when comparing Figures VI-4(a) and III-1(a) for the 24-inch

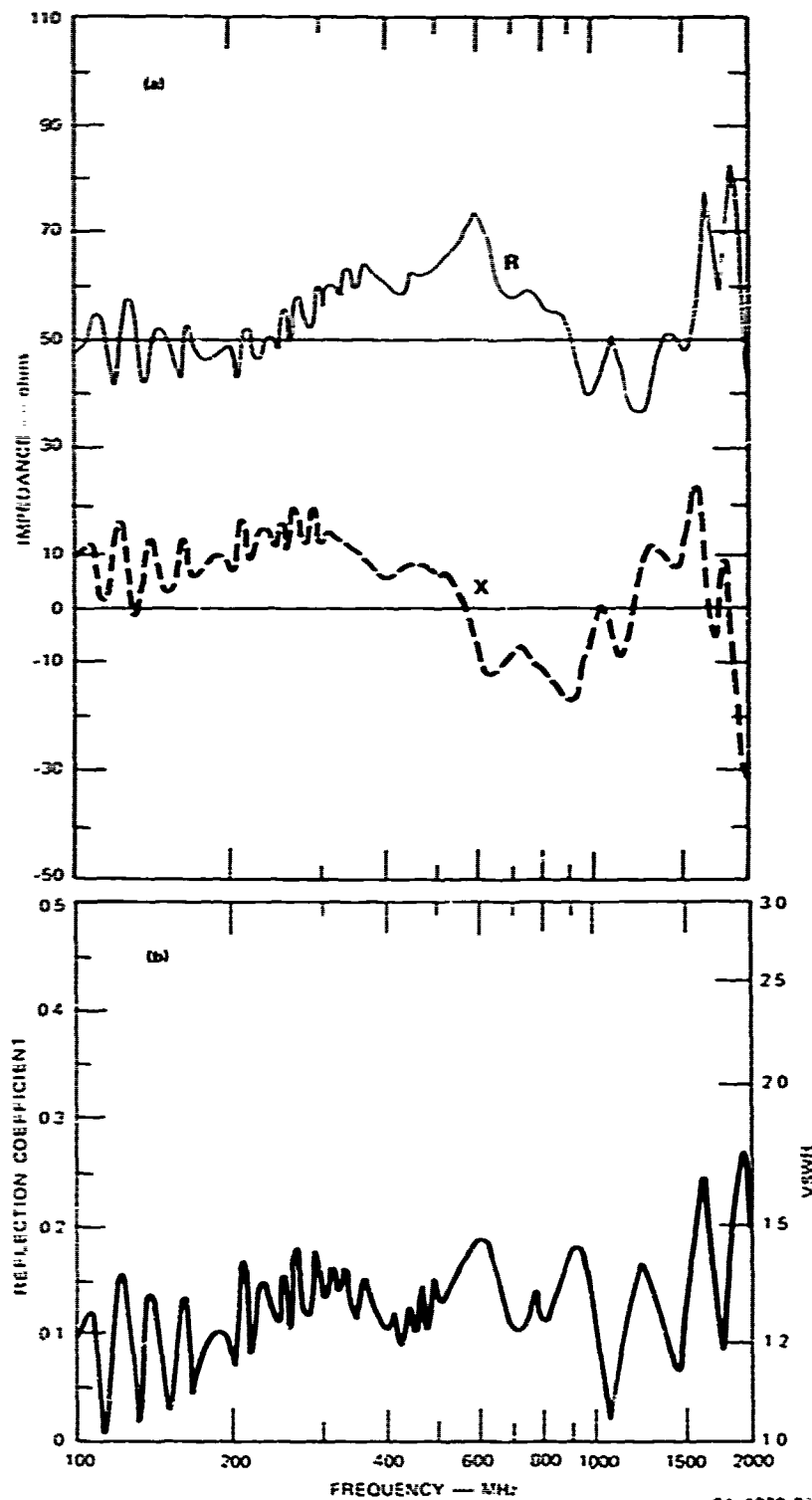
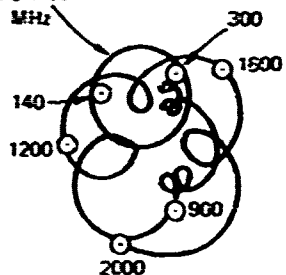


FIGURE VI-4 IMPEDANCE AND REFLECTION DATA AT THE UNBALANCED TERMINAL OF THE COMPACT BALUN CONNECTED TO THE 24-INCH SPIRAL ANTENNA BY MEANS OF A TRANSMISSION LINE PERPENDICULAR TO THE ANTENNA. The antenna is situated in free space. The transmission line is a 132-ohm twin-lead line of length approximately equal to the radius of the antenna.

CIRCLE CENTERED AT
 $1 + j0.2$ CONTAINING
 THE FREQUENCY POINTS
 FROM 140 TO 300 MHz



$\frac{Z}{50}$

SA-1370-28

FIGURE VI-5 SMITH-CHART PLOT OF THE IMPEDANCE DATA OF FIGURE VI-4.
 (Frequency range: 140-2000 MHz.)

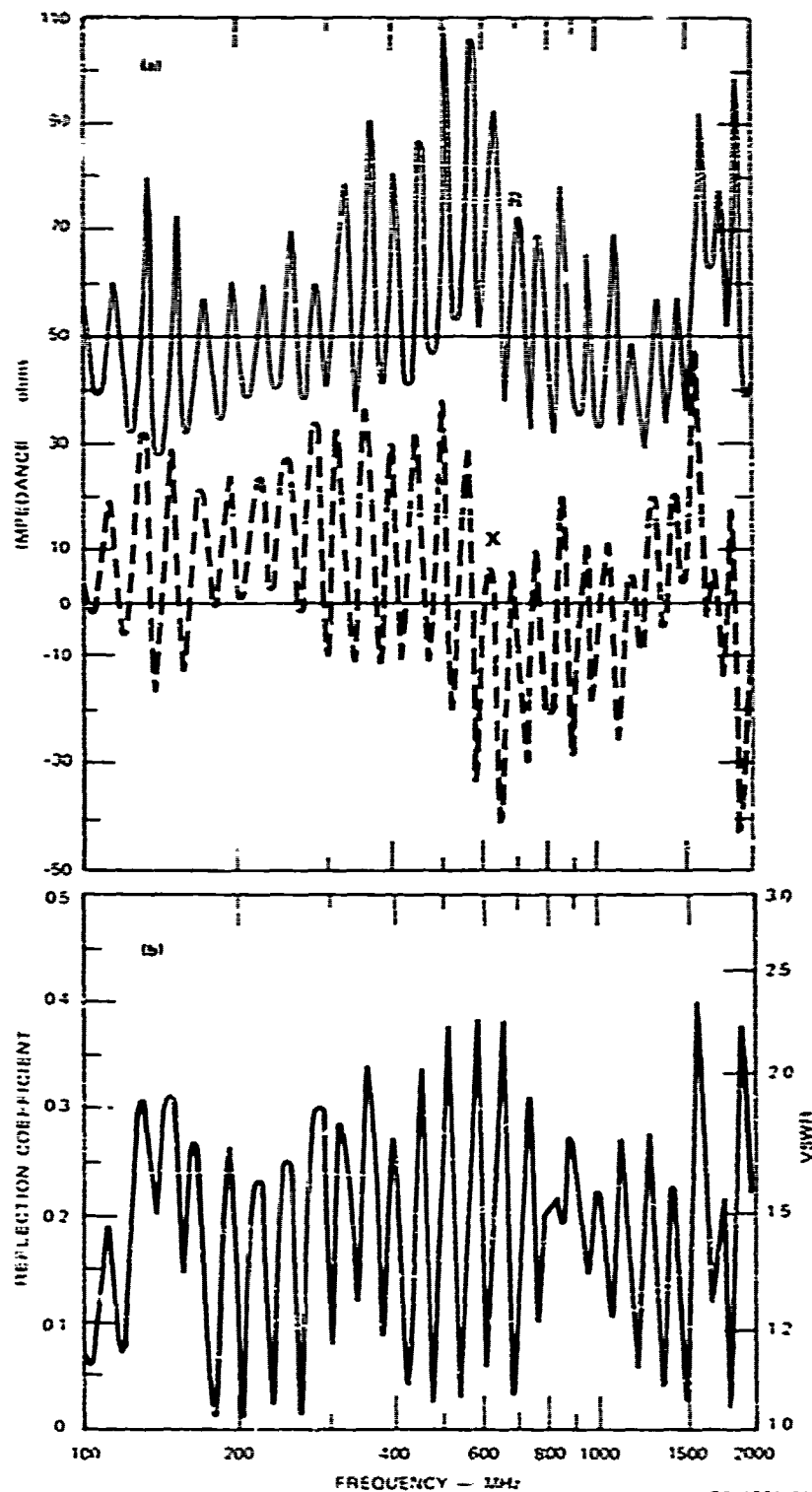
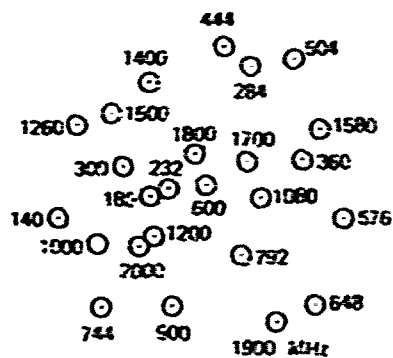


FIGURE VI-6 IMPEDANCE AND REFLECTION DATA AT THE UNBALANCED TERMINAL OF THE COMPACT SALUN CONNECTED TO THE 24-INCH SPIRAL ANTENNA BY MEANS OF A TRANSMISSION LINE PARALLEL TO AND TOUCHING THE ANTENNA ($d = 0.078$ inch, Figure IV-1). The antenna situation and transmission-line type are the same as indicated for Figure VI-2



50/21

SA-1579-30

FIGURE VI-7 SMITH-CHART PLOT OF THE IMPEDANCE DATA OF FIGURE VI-6.
(Frequency range: 140-2000 MHz.)

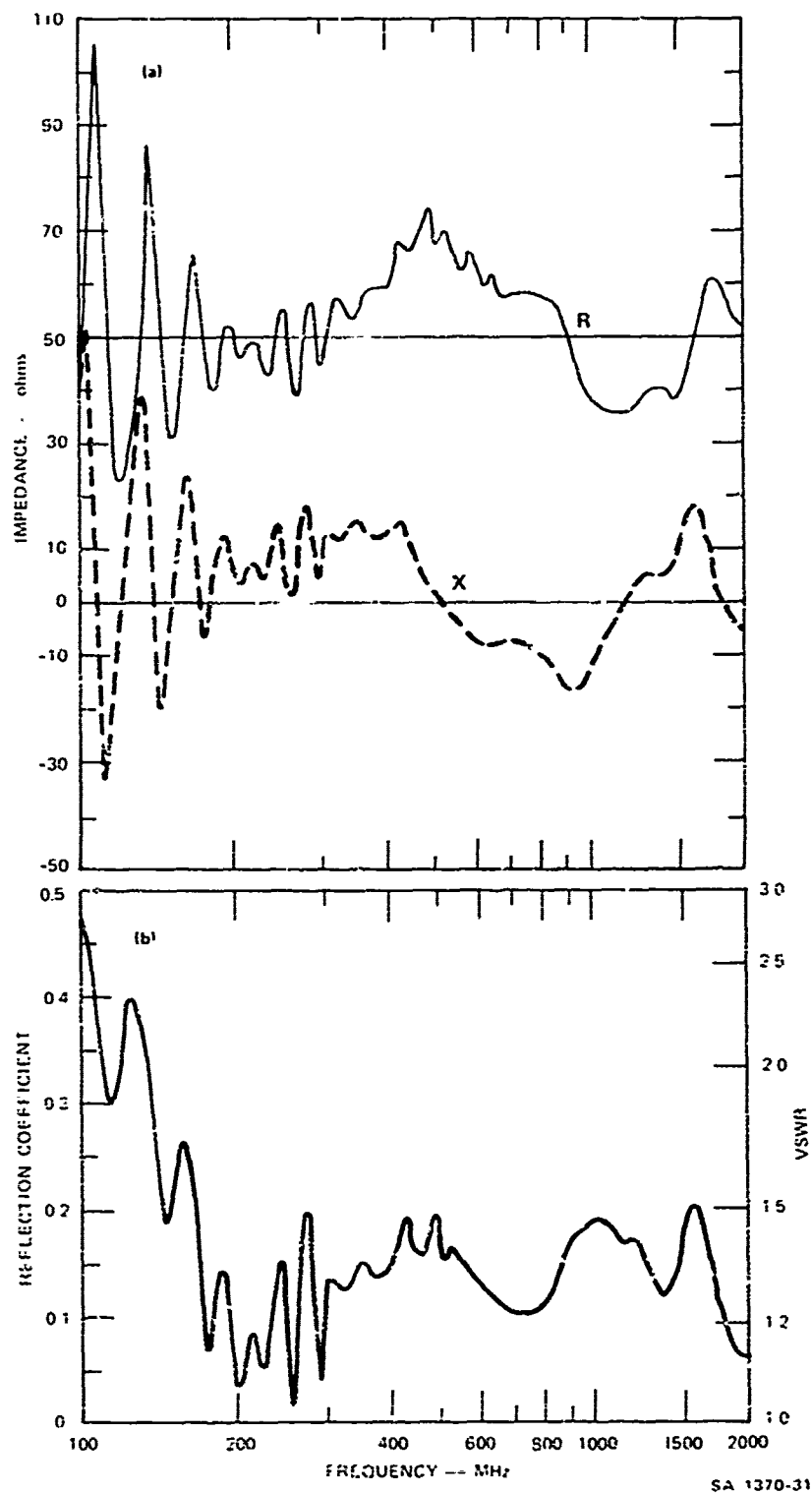
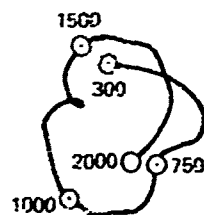


FIGURE VI-8 IMPEDANCE AND REFLECTION DATA AT THE UNBALANCED TERMINAL OF THE COMPACT BALUN CONNECTED TO THE 12-INCH SPIRAL ANTENNA BY MEANS OF A TRANSMISSION LINE PERPENDICULAR TO THE ANTENNA. The antenna situation and transmission-line type are the same as indicated for Figure VI-4.



$\frac{Z}{50}$

SA-1370-32

FIGURE VI-9 SMITH-CHART PLOT OF THE IMPEDANCE DATA OF FIGURE VI-8.
(Frequency range: 300-2000 MHz.)

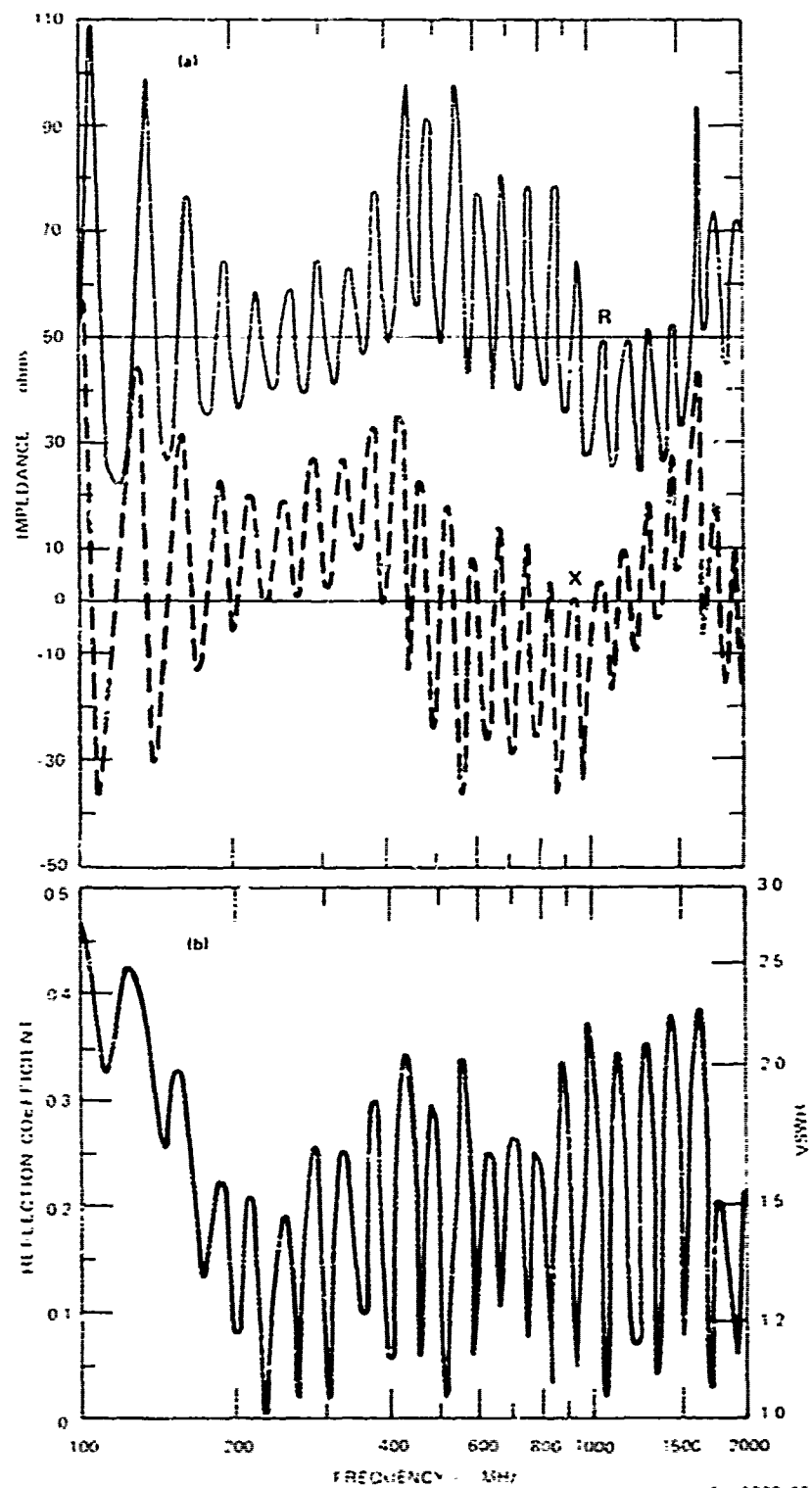
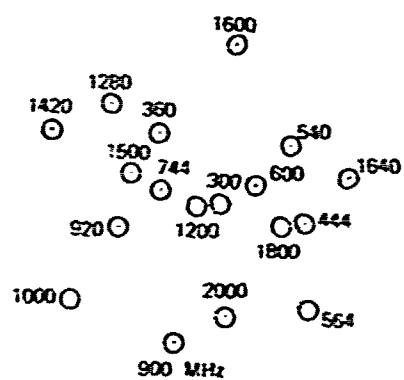


FIGURE VI-10 IMPEDANCE AND REFLECTION DATA AT THE UNBALANCED TERMINAL OF THE COMPACT BALUN CONNECTED TO THE 12-inch SPIRAL ANTENNA BY MEANS OF A TRANSMISSION LINE PARALLEL TO AND TOUCHING THE ANTENNA (d = 0.078 inch, Figure IV-1). The antenna situation and transmission line type are the same as indicated for Figure VI-2



$\frac{Z}{50}$

SA-1370-34

FIGURE VI-11 SMITH-CHART PLOT OF IMPEDANCE DATA OF FIGURE VI-10.
(Frequency range: 300-2000 MHz.)

antenna and Figures VI-8(a) and III-7(a) for the 12-inch antenna. It is seen from these figures that the average driving-point impedances (balanced) are brought down to around an average 50-ohm impedance (unbalanced) over the radiating frequency range of the antennas. Over this range the impedances do vary with frequency about the 50-ohm impedance line (or the center of the Smith charts shown in Figures VI-5 and VI-9). Comparing Figures VI-4(a) and VI-8(a) with Figure V-4, it is seen that these variations for each antenna follow closely the impedance characteristic of their respective balun (Balun A with the 12-inch antenna, and Balun B with the 24-inch antenna). The effect of appropriately terminating the antennas is also seen when comparing Figures VI-4(a) and VI-8(a) with III-1(a) and III-7(a). Here it is noted that the impedance of both balun/antenna configurations is maintained close to 50 ohms at frequencies below the radiating frequency band. For the 24-inch-antenna configuration, a match to a 50-ohm system with VSWRs less than 1.4 is achieved at frequencies down to 100 MHz. This is to be compared to 140 MHz, which is the low-frequency limit of the radiating frequency band of the 24-inch antenna. For the 12-inch antenna, a match with VSWRs less than 1.5 is achieved at frequencies down to 175 MHz. This is compared to the low-frequency, radiating-frequency-band limit of 300 MHz. If the antennas had not been terminated, the match at frequencies below the radiating-frequency band of each antenna would have been degraded significantly. In both cases, VSWRs on the order of 5:1 would be observed even after accounting for the balun impedance transformation.

Figures VI-6 and VI-7 for the 24-inch antenna and Figures VI-10 and VI-11 for the 12-inch antenna show the effect on the impedance of the balun/antenna configurations when the transmission lines connecting the baluns to their respective antennas are brought in close contact with the antennas. As would be expected from the results discussed in

Section IV, significant impedance fluctuations occur with frequency. The average impedance characteristic exhibited in this case is essentially the same as for the case in which the transmission line is perpendicular to the antenna except that the impedance fluctuates rapidly with frequency in a log-periodic manner. This, as explained in Section IV, is because the fields excited by the antenna interact with the transmission line. Over the frequency range that includes the radiating-frequency band and the frequency range in which the antenna terminations are effective in preventing reflections from the outer ends of the antenna, VSWRs as high as 2.3 are observed relative to 50 ohms. As discussed below, however, the maximum loss in system sensitivity of this low-profile balun-antenna configuration is small compared to the perpendicular-transmission-line configuration, amounting to only about 0.7 dB for both antennas.

The above results are summarized quantitatively in Table VI-1 for the 24-inch-antenna configurations and Table VI-2 for the 12-inch-antenna configurations. The peak VSWR and the system sensitivity loss caused by reflections are shown for both the balun/antenna configurations and for the antenna alone, driven by a hypothetical, 50-ohm, balanced generator at the spiral center. Peak VSWR was determined over the frequency range for which a reasonably good system-to-antenna impedance match was maintained. For the two balun/antenna configurations, this frequency range extended below the radiating band because the antennas were terminated. System sensitivity loss is based on the peak VSWR occurring over the radiation band of the antennas: it reflects only the loss resulting from the system-to-antenna mismatch and does not account for the loss (about 0.6 dB) introduced by the compact baluns used in the balun/antenna configurations. The upper frequency limit for which peak VSWR and system sensitivity loss was determined is 500 MHz above the specified operating frequency of the two antennas. From the tables

Table VI-1

PEAK VSWR AND SYSTEM SENSITIVITY LOSS
FOR SEVERAL 24-INCH ANTENNA CONFIGURATIONS*

Configuration	Corresponding Figures	Peak VSWR Over the Frequency Range for Which the Antenna Impe- dance is Matched to the System Impedance	System Sensi- tivity Loss Due to Reflection Over the Radia- ting Frequency Band of the Antenna (dB)
Balun connected to antenna by means of transmission line perpendicular to antenna	VI-4, VI-5	1.7	0.3
Balun connected to antenna by means of transmission line parallel to and touching antenna	VI-6, VI-7	2.3	0.7
Antenna driven by a hypothetical. 50-ohm. balanced generator at the spiral center	III-1, III-2	3.1	1.3

* VSWR is shown relative to a system impedance of 50 ohms.

* 100 to 2000 kHz when the antenna was terminated. 140 to 2000 kHz when the antenna was not terminated.

Table VI-2

**PEAK VSWR AND SYSTEM SENSITIVITY LOSS
FOR SEVERAL 12-INCH ANTENNA CONFIGURATIONS***

Configuration	Corresponding Figures	Peak VSWR Over the Frequency Range for Which the Antenna Impe- dance is Matched to the System Impedance	System Sensi- tivity Loss Due to Reflection Over the Radia- ting Frequency Band of the Antenna (dB)
Balun connected to antenna by means of transmission line perpendicular to antenna	VI-8, VI-9	1.5	0.2
Balun connected to antenna by means of transmission line parallel to and touching antenna	VI-10, VI-11	2.2	0.7
Antenna driven by a hypothetical 50-ohm, balanced generator at the spiral center	III-7, III-8	3.1	1.2

* VSWR is shown relative to a system impedance of 50 ohms.

* 175 to 2000 MHz when the antenna was terminated. 300 to 2000 MHz when the antenna was not terminated.

and the previous data presented in this section, it is seen that up to frequencies as high as 2000 Mc both antennas still radiate and maintain an acceptable match with a 50-ohm system.

It is seen from Tables VI-1 and VI-2 that loss of system sensitivity due to the close proximity of the balun-to-antenna transmission line to the spiral conductors is not of major significance. From the standpoint of system sensitivity, then, it would make little difference which balun/antenna configuration was used. A good antenna-to-system match is important, however, if amplitude and phase distortions of the signal are to be minimized. Such distortions will degrade the information content of a signal. Signal phase and amplitude distortions may occur because a mismatch between antenna and the rest of the system can create a signal multibounce condition. Also, if the mismatch (VSWR) varies rapidly with frequency, the phase and amplitude of a signal passing through the antenna will be varied with frequency. Multibounce can occur between the antenna and objects close to the antenna that reflect electromagnetic energy. Multibounce can also occur within a coaxial cable connecting the balun to the system if the cable is not matched properly at both ends. In the latter case, if the cable is relatively lossless, resonances can occur when the cable length is a multiple of a half-wavelength of the signal frequency. It is the returning multibounce signal that interferes with the incident signal to cause signal distortion. It is noted that the effects of multibounce could be somewhat greater for the balun antenna configuration with the parallel transmission line than for the perpendicular-transmission-line configuration.*

* From the peak VSWR values given in Tables VI-1 and VI-2, it is seen that the maximum reflected signal strength that can occur for the parallel-transmission-line configuration is about 8 dB down from the incident signal strength, and for the perpendicular-transmission-line configuration, about 13 dB down.

but signal distortion is more apt to occur with the former configuration because of the rapid change of VSWR with frequency at the unbalanced port of its balun (see Figures VI-6(b) and VI-10(b)).

In conclusion, it is seen from the data presented in this section that the match of the antenna driving point impedance to a 50-ohm system impedance is improved significantly by use of the compact balun. The balun serves not only as an impedance transformer but as an unbalanced to balanced line transformer as well. Furthermore, this match improvement was extended to frequencies below the radiating frequency band of the antenna with use of combination lumped and distributed loads terminating the outer ends of the antennas. These terminations were effective in absorbing signals reaching the outer ends of the antennas in the frequency range of 100 to 140 MHz for the 24-inch antenna and 175 to 300 MHz for the 12-inch antenna.

It is also seen, however, that the low-profile balun antenna configuration does not match as well to a 50-ohm system, over the extended frequency range, as does the balun/antenna configuration that includes the transmission line perpendicular to the antenna. For the low-profile configuration, the VSWR peaks are larger and more frequent. This impairment in the antenna-system match causes little additional system-sensitivity loss, but can result in signal distortion. The effects of multibounces are greater for the low-profile configuration than for the perpendicular-transmission-line configuration because stronger signals are reflected at the point of mismatch. Furthermore, because of the transmission-line interaction with the radiated fields of the low-profile antenna configuration, the VSWR at the connection between the system and the balun varies rapidly with frequency, causing phase and amplitude distortions that contribute in addition to any distortion due to multibounce. Whether or not signal distortion (loss

of information) will prove to be serious depends on the environment under which the antenna system will have to operate. The frequency of the received signal, its bandwidth, and the kind of information desired from the signal must be considered. The low-profile-configuration impedance match can be improved (with the reduction of signal distortion) by moving the transmission line away from the antenna. This, of course, is done at the expense of the low profile of the balun/antenna configuration.

VII SUMMARY AND CONCLUSIONS

The input impedance at the center terminals has been measured for two planar equiangular spirals printed on a dielectric sheet. The spirals are self-complementary except near their centers and over the outside quarter turn, and are free to radiate on both sides of the plane of the spiral. When making most of the measurements, the antennas were placed against various building materials. Based on the average input impedance within the frequency band for good radiation from each antenna, two baluns have been designed and constructed to provide a good match between the antennas and 50-ohm coaxial transmission lines. These baluns have been combined with the spiral antennas to form a thin package, and impedance measurements have been made for the balun/antenna combination.

The data presented in this report show that the input impedance at the spiral center is hardly affected by placing the dielectric side of the antenna against dielectric building materials. (Solid metal and materials containing large amounts of metal were specifically excluded from the choice of building materials.) This insensitivity of impedance to the environment is related to the fact that the dielectric sheet supporting each spiral is sufficiently thick that the local fields near the center feed points do not penetrate significantly through the dielectric sheet. The resistive part of the input impedance, averaged over the radiating frequency band, is 125 ohms for the 24-inch-diameter spiral, and 137 ohms for the 12-inch-diameter spiral. These are lower than the theoretical value of $377/2 = 188$ ohms because of the presence of the dielectric sheet on which each spiral is printed and because of

the finite conductor thickness to-spacing ratio. The reactive part of each input impedance is low over the radiating-frequency band.

The low-frequency cutoff of the frequency band for efficient radiation was found to be affected by the materials placed near the antennas. The low-frequency cutoff is determined by the circumference of the outside of the antenna being about a wavelength for the currents propagating along the spirals. The fields in the radiating region of the antenna do, of course, extend through the support dielectric into the building materials. The building materials thus change the effective wavelength on the spiral. The largest measured change occurred when the 24-inch spiral was moved from free space to a position against a plastered brick wall, which lowered the cutoff frequency from 140 to 110 MHz. The corresponding frequencies for the 12-inch spiral are 300 and 250 MHz.

A unique feature of the compact baluns designed and built for these spiral antennas is that the impedance transformation ratio is other than 4:1 or 1:1. These baluns have peak VSWRs very close to the limit set by the miniature ferrite cores. The ferrite material used is the best suited to the application. Some improvement might be possible by using larger toroids, but at the expense of increasing the balun size. When terminated with a 132-ohm balanced resistive load (which is the average of the two antenna impedances), the compact baluns have VSWR < 1.35 over the 100-to-2000 MHz band over which measurements were made.

The compact baluns constructed are as thin as is consistent with the SMA (OSM) coaxial connector used. The clearance to a mounting surface is just adequate to clear the coupling nut as a connector is screwed onto the balun. If no connector was used on the balun, but a miniature coaxial cable was permanently soldered to the balun, then the balun thickness could be reduced further to on the order of 1/8 inch.

The outside ends of the spiral conductors must be terminated if there is to be low VSWR at the center input terminals when the drive frequency is below the low-frequency-radiation cutoff. Distributed loss is necessary to give good VSWR immediately below cutoff, and a lumped network is required to give good VSWR far below cutoff. For example, the input match of the unterminated 12-inch spiral quickly degraded to $VSWR \approx 10$ as the frequency was reduced below 300 MHz. With the termination in place, that antenna has $VSWR < 1.5$ down to 165 MHz, and $VSWR < 3$ at 100 MHz. Further improvement is probably possible.

Making the combination of each antenna and balun as flat as possible required some compromise of the electrical performance. From the electrical viewpoint, the transmission line that feeds the antenna center should be placed so that it interacts very little with the antenna fields. It is not practical to route the feeding transmission line along the spiral conductors of these antennas because the width of the conductors near each antenna center is very narrow, and because the length of line required would have significant dissipation loss. Keeping the feed line several inches from the antenna surface gives good input VSWR, but is inconsistent with the desire for a flat structure. The configuration finally adopted has the balun mounted at the antenna periphery, with a miniature two-wire line running from the balun to the antenna center terminals. The interaction between the antenna fields and the two-wire line produces many peaks of up to $VSWR = 2.3$ for the antenna and balun combinations. This represents a maximum power loss of 0.7 dB due to mismatch when the antenna is used with a 50-ohm system, which is only 0.5 dB greater mismatch loss than if the balun-to-antenna two-wire line were mounted far from the antenna surface.

REFERENCES

1. L.A. Robinson, "Impedance Measurement and Matching for Spiral Antennas," Final Report, Contract 1083-100623-SCC-09824, SRI Project 1081, Stanford Research Institute, Menlo Park, California (June 1971).
2. Ibid., Sec. II-B.
3. Ibid., Sec. II-C.
4. Hewlett-Packard 8540 Series Programmer's Software Manual, HP Publication 08542-90015, Section 3-6 (August 1969).
5. F.L. ReQva, "Resistance and Capacitance Relations Between Short Cylindrical Conductors," Trans. AIEE, Vol. 64 (October 1945).
6. R. Sivan-Sussman, "Various Modes of the Equiangular Spiral Antenna," IEEE Trans. on Antennas and Propagation, Vol. AP-11, pp. 533-539 (September 1963).
7. L.A. Robinson, op. cit., Sec. I.
8. V.H. Rumsey, Frequency Independent Antennas, Sections 3.2 and 4.3. (Academic Press, New York, N.Y., 1966).
9. G.L. Matthaei, Leo Young, and E.M.T. Jones, Microwave Filters, Impedance-Matching Networks, and Coupling Structures, Section 4.09 (McGraw-Hill Book Co., New York, N.Y., 1964).

Preceding page blank